JCGB Vol. 2 No. 1 (2025)

Journal of Computational Genomics and Biology

journal homepage: https://fargroups.com/index.php/JCGB/index

A m1A- , *m5C*- , m6A- and m7G- regulators-related lncRNA Signature as a Prognostic and Immune-infiltrated Model for Lung Adenocarcinoma

Li Shan[a,b], Er-Dong Zuo[b], Lian Lian[c,*], Xu Cheng[b,*]

[a]Yangzhou University, Jiangsu 215100, China
[b]Department of Radiotherapy Oncology, The First People's Hospital of Taicang, Jiangsu 215400, China
[c]Department of Oncology,Suzhou Xiangcheng People's Hospital, Xiangcheng Clinical School, Yangzhou University Medicine Colloge

*Correspondence:
Lian Lian: dr-lianlian@163.com
Xu Cheng: chx1029@163.com

Funding

The authors acknowledge the financial grant by the basic research program for medical and health applications of the Taicang Science and Technology Bureau of Jiangsu Province(grant numbers TC2023JCYL15).

Abstract

Lung adenocarcinoma (LUAD) is the most common subtype of lung cancer worldwide. Many patients still do not benefit from multitargeted antitumor therapy, even in combination with immunotherapy. m6A-/m1A-/m5C/-m7G- regulators are the major forms of RNA methylation (RM) modification. development is closely related. This study summarizes 64 m6A-/m1A-/m5C/-m7G regulators. Based on the transcriptomic data and clinical information of LUAD in the Cancer Genome Atlas (TCGA), the role of prognosis RNA methylation modification-regulated lncRNAs (RM-lncRNAs) in LUAD and microenvironment was explored. To identify

RM-lncRNAs and how they affect survival and prognosis in LUAD, we constructed signatures of RM-lncRNAs by univariate and multivariate regression and least absolute shrinkage and selection operator (LASSO) analysis. Penalized regression was used to screen and establish a prognostic model closely related to the subgroup of clinical variables and the degree of immune cell infiltration, and the risk score of each sample was calculated independently. Using Kaplan-Meier (K-M) analysis, gene enrichment analysis and multi-pathway clinical correlation analysis, the clinical significance and potential mechanism of action of the prognostic model were elucidated, including PLUT, AC091133.4, AC079949.2, and AC068338.3. At the same time, the high mutation frequency genes significantly associated with high risk in the prognostic model were further analyzed in combination with the incidence of somatic mutation of TCGA-LUAD. The risk score and consensus clustering generated by this prognostic model can effectively predict the clinical outcome and immune microenvironment infiltration characteristics of LUAD patients from multiple approaches and multiple methods. The above comprehensive data support the potential clinical application value of our constructed RM-lncRNA signature in the prognosis and immune infiltration status of LUAD. The purpose and originality of this study lies in revealing the potential link between RM modification patterns and LUAD and treatment response by constructing the LUAD prognostic model of RM-lncRNAs. This novel RM-lncRNA prognostic model can be used to assess the prognosis and sensitivity of infiltrating immune cells modulated by immunotherapy in patients with LUAD.

Keywords: Lung adenocarcinoma (LUAD); m1A; m5C; m6A; m7G; RNA Methylation (Rm); Lncrna; Prognostic Model; Immunotherapy

1. Introduction

Lung cancer is still currently fatal disease, which at a high level of mortality. There are an estimated 2.09 million new cases and 1.76 million deaths each year. To make matters worse, lung cancer incidence and mortality are on the rise. The pathogenesis of Lung adenocarcinoma (LUAD), the largest subtype of lung cancer, is complex, and

RNA methylation (RM) may be one of the pathogenesis of LUAD. Recently, many studies have shown that aberrant RM modifications are involved in LUAD. As the most abundant modification [1–3], RNA post-transcriptional modification has been considered as an important process in epigenetic regulation [4]. Mechanistically, more than 70 RMs occurs in mRNA and ncRNA in various tumors across species [5,6]. it plays a role in regulating gene expression such as RNA stability, localization, mRNA translation and translocation by affecting chromatin structure, DNA conception, stability, and protein interaction [7,8]. Different methylation sites exist in different forms of RM [9]. Recent studies have shown that modifications such as N6-methyladenosine (m6A) [10,11], N1-methyladenosine (m1A) [12,13], 5-methylcytosine (m5C) [14] and 7-methylguanosine (m7G) [15], which are widespread in transcriptomic RNA [16], have been shown to be involved in a variety of human diseases play a broad and profound role [17]. RM regulators have potential roles on diagnosis, prognosis and treatment strategies of LUAD [18,19]. However, the prognostic value of RM-related lncRNAs (hereinafter referred to as RM-lncRNAs) [20] in LUAD is unclear yet. m6A-modified lncRNAs were found in eukaryotic mRNAs and lncRNAs to play indispensable roles in the course of various malignancies [21]. For example, FEZF1-AS1, which is affected by RNA modification, through the action of ITGA11/miR-516b-5p regulates the ITGA11/miR-516b-5p axis and is ultimately lead to the evolution of NSCLC [21,22]. In addition, as the target of METTL3, ectopic expression of ABHD11-AS1 caused poor prognosis in NSCLC [23]. Studies have shown that RM exists in the key regulations of a variety non-coding RNAs. Moreover, the regulatory effect of lncRNA is closely related to spatial expression, and its abnormal regulation often affects the development and progression of cancer. Studies such as these suggest a specific role for RM modifications. Dysregulation of lncRNAs is associated with LUAD prognosis. It may act as a signal molecule, or a mediator to recruit other regulatory factors to exert the function of regulating gene expression on target genes. However, the distribution, functions and roles of RM modifications in lncRNAs are still poorly understood. Therefore, RM-lncRNA regulators have crucial applications in the underlying mechanisms

leading to tumor progression and the efficiency of immunotherapy responses [24].

As important as its clinical significance, the tumor microenvironment (TME), as the environment for tumor survival, is the soil for tumor growth, migration and invasion [25–28]. During tumorigenesis, TME recruits immune cells and serve as environmental drivers of tumor growth and metastasis to a certain degree as an environmental driver of malignancy. However, the modification mechanisms of lncRNAs currently focused on tumor progression and immune cell infiltration in the TME remain unclear. The excellent antitumor effect of immunotherapy in malignant tumors has already abounded [29–31]. As research progresses, in addition to many ICIs similar to PD-L1, the heterogeneity of TMB, dMMR, and even MSI-H can also be used as immunotherapy biomarkers [32,33]. Therefore, the purpose of our research is to find more and more effective biomarkers to guide the prognosis of LUAD and predict the efficacy of immunotherapy regimen.

In this study, 64 m6A-/m1A-/m5C-/m7G-related genes were summarized with data of 59 normal samples and 535 LUAD samples in TCGA. Differentially expressed RM regulators in LUAD were screened with LASSO-Cox algorithm and K-M survival analysis. A threshold of $|cor| > 0.3$ was used to identify 210 prognosis related RM-lncRNAs for LUAD prognostic signature construction. Forty-five differential RM-related lncRNAs affecting the prognosis of LUAD were obtained by univariate regression analysis related to overall survival (OS). Further prognostic LASSO-Cox regression obtained a prognostic model composed of four lncRNAs, which were used as lncRNA markers associated with RM regulators of LUAD. Subsequently, Cox regression analysis was performed by combining 485 samples with complete clinical information, and it was confirmed that the high-risk group had a shorter OS time and was associated with poor prognosis in various clinical subgroups. Consistent clustering based on the RM-lncRNAs prognostic model also showed significant differences between groups. The above results suggest that the RM-lncRNAs prognostic model is an independent prognostic factor for predicting OS. Then, a PPI interaction network was constructed for the differentially expressed lncRNA prognostic model related differentially expressed lncRNA genes between the high and

low risk groups, and GO, KEGG and Gene Set Enrichment Analysis (GSEA) were performed. Our study proposes a LUAD prognostic marker with clinical reference value based on potential prognosis-related lncRNAs associated with RM modifications. This study deepens the understanding of TME status in LUAD patients and lays a theoretical foundation for the selection of immunotherapy.

2. Methods

2.1. Data collection and processing

Transcriptome and simple nucleotide variation data were downloaded from TCGA (https://cancergenome.nih.gov/), and the expression data of 594 LUAD patients were compared downloaded. for LUAD patients were downloaded from TCGA was calculated.

2.2. Identification of RM regulator-related lncRNAs and analysis of their prognostic value

By consulting the latest literature, a total of 64 m6A-, m1A-, m5C-, m7G-RM regulator-related genes were obtained. Including 4 m1A-RM regulators (TRMT61A, TRMT61B, TRMT10C, TRMT6), 21 m5C-RM regulators (ALYREF, DNMT1, DNMT3A, DNMT3B, DNMT3L, NSUN2, NSUN3, NSUN4, NSUN5, NSUN5P1, NSUN6, NSUN7, TET1, TET2, TET3, TP53, TRDMT1, YBX1, YBX2, YBX3, YTHDF3-AS1), 37 m6A-RM regulators [34,35] (METTL3, METTL14, WTAP, VIRMA, ZC3H13, CBLL1, RBM15, RBM15B, METTL16, ZCCHC4, PCIF1, FTO, ALKBH5, ALKBH3, YTHDF1, YTHDF2, YTHDF3, YTHDC1, YTHDC2, HNRNPA2B1, HNRNPC, RBMX, IGF2BP1, IGF2BP2, IGF2BP3, FMR1, PRRC2A, EIF3A, LRPPRC, SRSF3, NXF1, TRMT112, NUDT21, CPSF6, SETD2, SRSF10, XRN1), and two m7G-RM regulators (METTL1, WDR4). Differentially expressed RM regulators in tumor and normal tissues in the TCGA-LUAD cohort were identified. 210 RM-lncRNAs with standard correlation coefficient ($|cor| > 0.3$ were obtained by Pearson correlation analysis.

2.3. Construction and validation of LUAD prognostic signatures of RM-lncRNAs

The TCGA-LUAD cohort was randomly divided into 1:1. Between training and testing groups, LASSO-Cox regression [36] analysis was used to build an RM-lncRNA signature, which named RMlncscore [37]. The formula is as follows: RMlnc-score = Σ (βi × Expi) (β: coefficient, Exp: lncRNA expression level). Then the patients were divided into high RMlnc score group and low RMlnc score group according to the median of RMlnc score. K-M survival curves [38] were drawn using the R package "survival", describing the OS difference between the high and low groups. ROC was used to evaluate its sensitivity and accuracy [39]. In addition, the RMlnc score was classified by sex (males and females), age (≤65 years and >65 years), T (T1-2 and T3-4), N (N0 and N1-2), relationship between M (M0 and M1/Mx) and prognostic power of each subgroup grade (stage I-II and stage III-IV). Then, through multivariate Cox regression analysis [40], nomogram [41] survival maps and calibration curves were constructed based on the 1-/3-/5-years survival probabilities of patients to further evaluate the prognostic value and clinical relevance of the model lncRNAs.

2.4. Establishment and validation of the prognostic gene signature

Combined with Cox and Lasso regression analysis, the penalized regularization parameter (λ) was chosen by the R package glmnet, n times equal to 10. Finally, survival analysis, scatterplots and heatmaps were performed in R software according to each patient's risk score. Time-dependent ROC curves reflects discriminating power by the area under the curve (AUC) [42]. Prognostic signature of RM-lncRNAs were validated by Cox regression, which incarnated independent prognostic factors via the 'forestplot' package in R. Nomograms and its corresponding were then built to drawn the clinical benefit.

2.5. Protein Interaction (PPI) network

We used a string-generated database (version 11.0) of DEGs reated to risk scores in the RM-lncRNAs prognostic model in the TCGA-LUAD dataset to construct a

molecular interaction network for analyzing closely interacting differential genes. Then, the PPI was exported, and the Cytoscape software was used for further analysis, the network properties of each node were calculated, and the MCODE [43] and Cytohubba [44] were used to mine the hub nodes based on the degree of the nodes. It may have an extremely important function in the modulation of the whole biological process, which deserves further study.

2.6. Comprehensive gene enrichment analysis

We performed GSEA [45], as well as GO [46] and KEGG [47], to reveal underlying molecular mechanism with risk score reated to RM-lncRNAs prognostic model. $P<0.05$ was considered significant and the graphs were constructed by the gplots package in R software.

2.7. Consistent clustering of prognostic RM-lncRNAs

Based on the constructed expression data of differentially expressed lncRNAs associated with RM regulators, “ConsensusClusterPlus" [48] was used to identify potential molecular subtypes. Prognosis of specimens of different molecular subtypes was analyzed using the R packages “survival" and “survminer”. Inclusion of clinical data and analysis of molecular subtype differences in different clinicopathological features.

2.8. Analysis and evaluation of immune cell infiltration

We analyzed immune cell infiltration by two integrated algorithms——CIBERSORT [49] and ESTIMATE [50]. Expression data were used to quantify the proportion of 22 TICs per sample using CIBERSORT. Meanwhile, ESTIMATE was used with default settings to determine immune and stromal cell content. to calculate the element in TME. At the same time, the Compositional infiltration differences with RM-lncRNAs prognostic model were compared in immune infiltration based on the clustering features of the RM-lncRNA prognostic model.

2.9. Statistical Analysis

All statistical analyses were performed using R software (v4.0.2). pvalues < 0.05 were considered statistically significant if not explicitly stated.

3. Results

3.1. Differential expression analysis of RM regulators in TCGA-LUAD

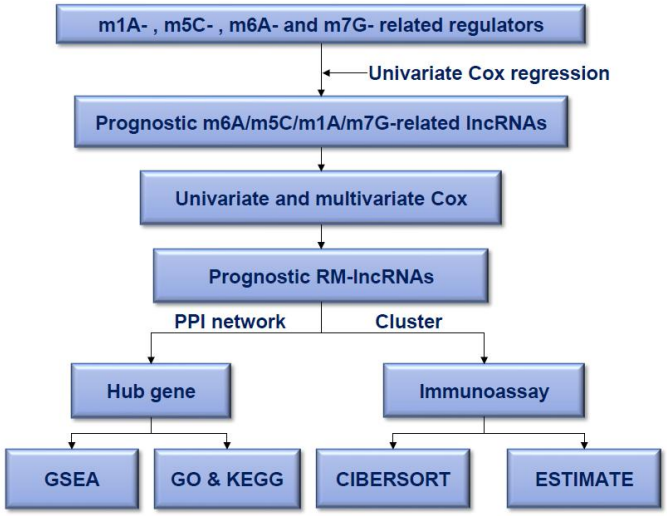

Fig. 1. Flowchart for constructing and validating a prognostic model for TCGA-LUAD OS.

The workflow of this study is shown in Fig. 1. We first performed gene differential expression analysis between normal samples and tumor samples in the TCGA-LUAD dataset, which was displayed in a volcano plot, and some genes with significant differential expression were marked in the figure (Fig. 2A). The Venn diagram showed |logFC|> 2 & adj.P < 0.05 as the threshold to screen the intersection of 142 differentially expressed genes (DEGs) and 64 m6A-/m1A-/m5C/-m7G- RM regulated genes, 24 differentially expressed RM regulators in LUAD were obtained (Fig. 2B). We then performed LASSO Cox regression analysis in the TCGA-LUAD dataset to obtain 8 RM regulators with prognostic significance for LUAD (Fig. 2C–D). We marked the differences with the differential ranking map (Fig. 2E), and reflected the group differences in gene expression through the differential expression heat map (Fig. 2F). At the same time, group comparison violin plots (Fig. 2G-H) show their differential expression in the TCGA-LUAD dataset.

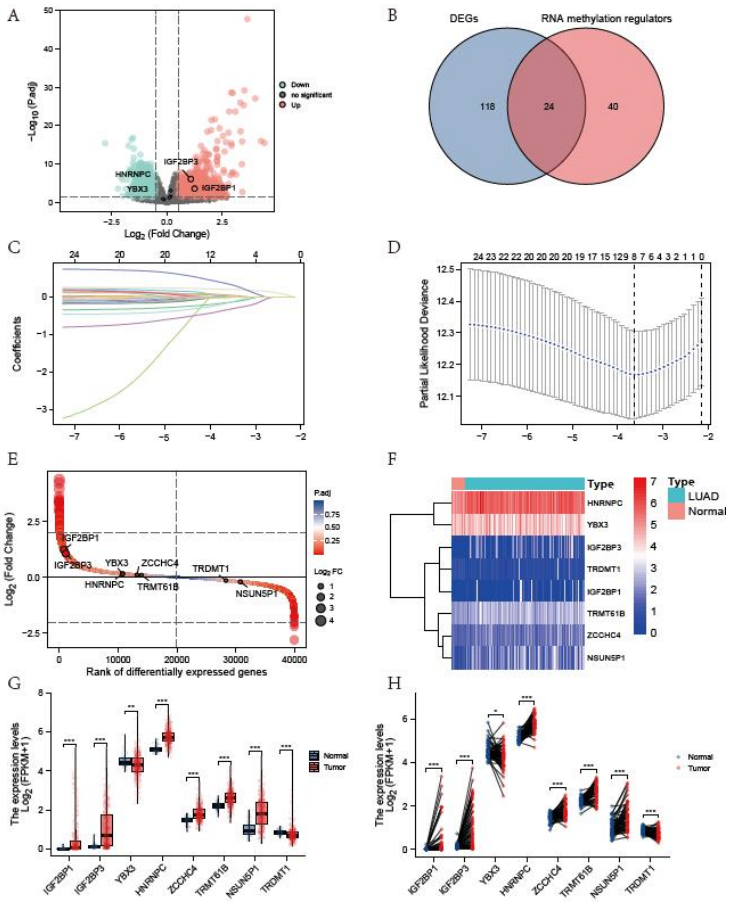

Fig. 2. Analysis of differential expression of RM regulators. (A) Volcano plot of gene differential expression analysis between normal samples and tumor samples in TCGA-LUAD dataset, some genes with significant differential expression are marked in the figure; (B) Venn diagram of intersection of 64 m1A-, m5C-, m6A- and m7G RM regulated genes and TCGA-LUAD dataset DEGs; (C-D) LASSO Cox regression analysis based on 24 differential RM regulated genes, found by least absolute contraction and selection operator (LASSO) cox regression 8 The best prognosis-related RM regulators; (E) Differential ranking map of RM regulators among DEGs in the CGA-LUAD dataset; (F) Heat map of differential expression of RM regulators Reflecting the differences in gene expression between groups; (G-H) Boxplots of differential expression between unpaired samples and paired samples of 8 differentially prognostic RM regulated genes in the TCGA-LUAD dataset.

3.2. Identification of RM regulator-related lncRNAs in LUAD patients

We performed KM OS analysis on 8 differentially expressed RM regulators that affected the prognosis and survival of LUAD patients, and plotted the survival curve, and found that HNRNPC, IGF2BP3, TRDMT1, and IGF2BP1 had significant statistical significance for OS in LUAD (Fig. 3A – D). We then analyzed lncRNAs

associated with 4 prognostic factors associated with RM regulators. 210 RM-lncRNAs with |cor| > 0.3 screened by Pearson correlation analysis were used for LUAD prognostic signature construction (Fig. 3E–G).

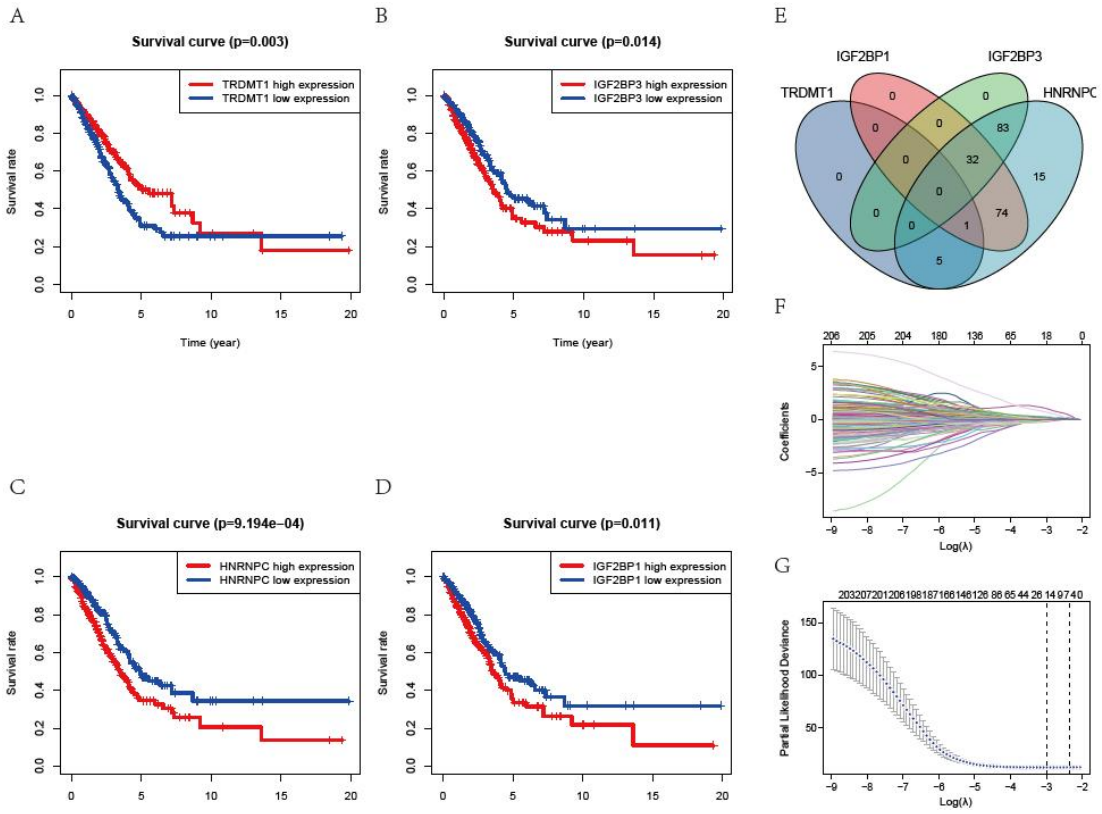

Fig. 3. Identification of lncRNAs associated with markers of prognostic RM regulators in LUAD patients. (A-D) TRDMT1, IGF2BP3, HNRNPC, and IGF2BP1 high and low expression groups have significant differences in the prognosis and survival of LUAD patients, which can be used as OS prognostic markers for LUAD; (E) Four LUAD OS prognosis were screened by Pearson correlation analysis 210 lncRNAs (|cor| > 0.3) associated with related RM regulators; (F-G) LASSO coefficient distribution map showing the results of 210 lncRNAs constructing LUAD prognostic signature analysis.

3.3. Construction and verification of m1A-, m5C-, m6A- and m7G- RM-lncRNAs prognostic signature in TCGA-LUAD

The above results suggested that RM modification-related lncRNAs may play an important role in LUAD. Therefore, we further investigated the prognostic features of RM modification-related lncRNAs in LUAD with univariate Cox regression analysis. Univariate Cox regression displayed 45 regulatory factors associated with patient

prognosis screened in 210 RM-lncRNAs by forest plot (Fig. 4A). Subsequently, regression coefficients of the 45 RM-lncRNAs associated with prognosis were calculated using LASSO Cox regression (Fig. 4B – C). We identified four RM-lncRNAs for forecast OS in LUAD, including PLUT, AC091133.4, AC079949.2, and AC068338.3. PCA plots were used to perform dimensionality reduction analysis between the two groups, suggesting that the risk score could well distinguish LUAD samples (Fig. 4D). We then calculated the 1-year, 3-year and 5-year AUCs based on the performance of the four RM-lncRNAs prognostic models by ROC curve test, which were 0.70 (0.78-0.63), 0.67 (0.73-0.60), 0.69 (0.77-0.61), respectively (Fig. 4E). Results showed that the risk model has a better prediction effect on the prognosis of LUAD (Fig. 4A). The K-M survival curve also suggested that the high-risk group was significantly associated with poor prognosis in LUAD (Fig. 4F). Multivariate Cox regression analysis was performed on the prognostic model to calculate the patient's risk score. The risk score, life status, and expression level distribution of the corresponding four RM-lncRNAs regulators in TCGA-LUAD are shown in Fig. 5A. Subsequently, we analyzed the predictive performance of RM-lncRNAs prognostic models - PLUT, AC091133.4, AC079949.2, AC068338.3 with the AUC of ROC, respectively PLUT (AUC = 0.653), AC091133.4 (AUC = 0.579), AC079949.2 (AUC = 0.619), AC068338.3 (AUC = 0.724) (Fig. 5B). At the same time, the significant expression differences of the RM-lncRNAs prognostic model between normal samples and LUAD samples in unpaired and paired samples were shown in box plots (Fig. 5C – D). Results suggested that AC068338.3 is low-expressed in tumor tissue, and AC079949.2, PLUT, and AC091133.4 are highly expressed in tumor tissue.

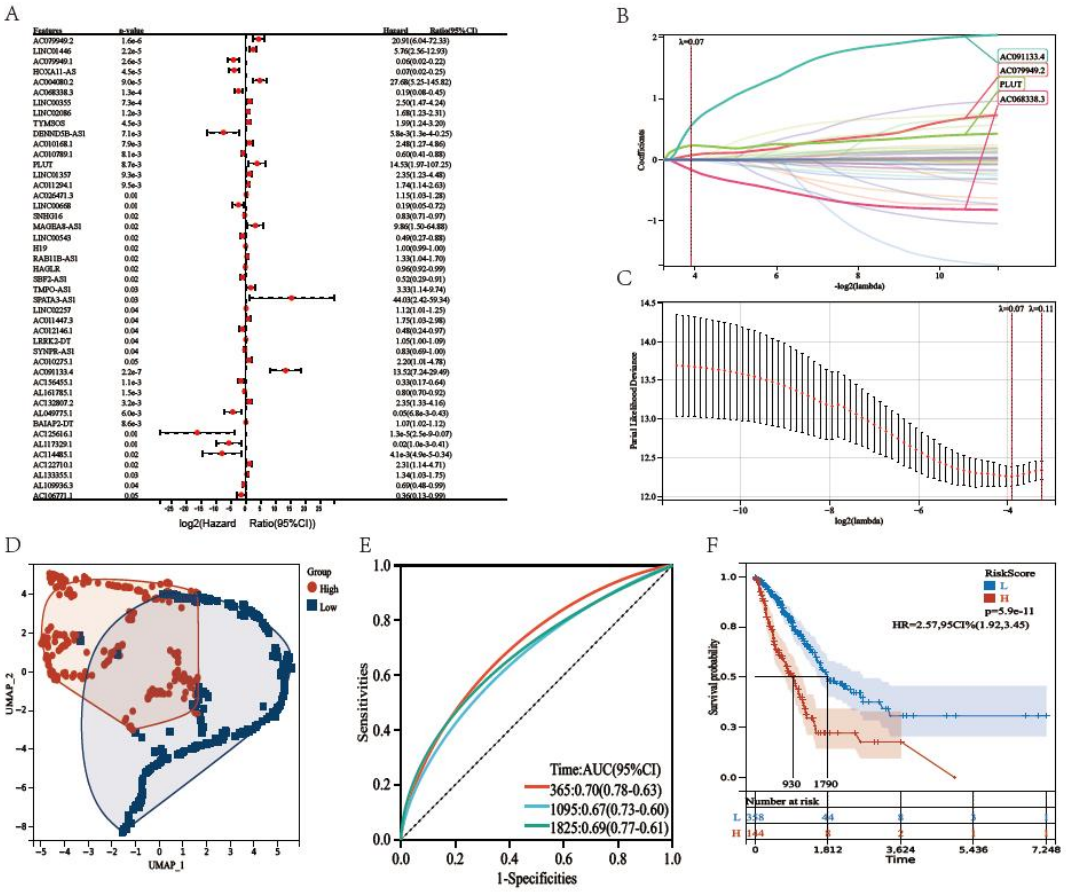

Fig. 4. Construction and verification of prognostic signature for RM-lncRNAs in TCGA-LUAD. (A) Forest plot of the univariate Cox regression analysis for RM-lncRNAs; (B-C) LASSO Cox coefficient profiles of the prognostic signature for RM-lncRNAs; (D) PCA graph dimensionality reduction analysis Evaluating the risk score can distinguish LUAD samples well; (E) AUC of the timeROC curve calculated the performance of the RM-lncRNAs prognostic model within 1 year, 3 years and 5 years; (F) The K-M survival curve also suggests that the high-risk group and LUAD have poor prognosis Significant correlation.

Next, we investigated whether the incidence of somatic mutations in TCGA-LUAD differed between high and low risk groups in the prognostic RM-lncRNA model. We used the chi-square test to assess differences in gene mutation frequencies in each group of samples. Among the 485 samples with complete clinical information, the genes with the highest mutation frequency in Top15 included TTN (p=2.0e-5), CSMD3 (p=1.6e-5), USH2A (p=1.7e-3), SPTA1 (p=2.4e-4), PCDH15(p=6.1e-3), PAPPA2(p=0.04), PCLO(p=0.02), RP1L1(p=8.2e-3), ZNF804A(p=0.01), HMCN1(p=0.02), NPAP1(p=3.5e-3), NRXN1(p=4.9e-3)), CACNA1E (p=7.1e-4),

ASPM (p=0.01), SORCS1 (p=0.02). The mutation frequencies were 58.3%, 47.8%, 39.8%, 30.1%, 23.4%, 21.8%, 21.8%, 20.7%, 19.6%, 18.8%, 18.3%, 18.0%, 17.5%, 16.7%, and 15.6%, respectively. We used the "maftools" software package to generate a mutational map, and presented a waterfall plot (Fig. 5E).

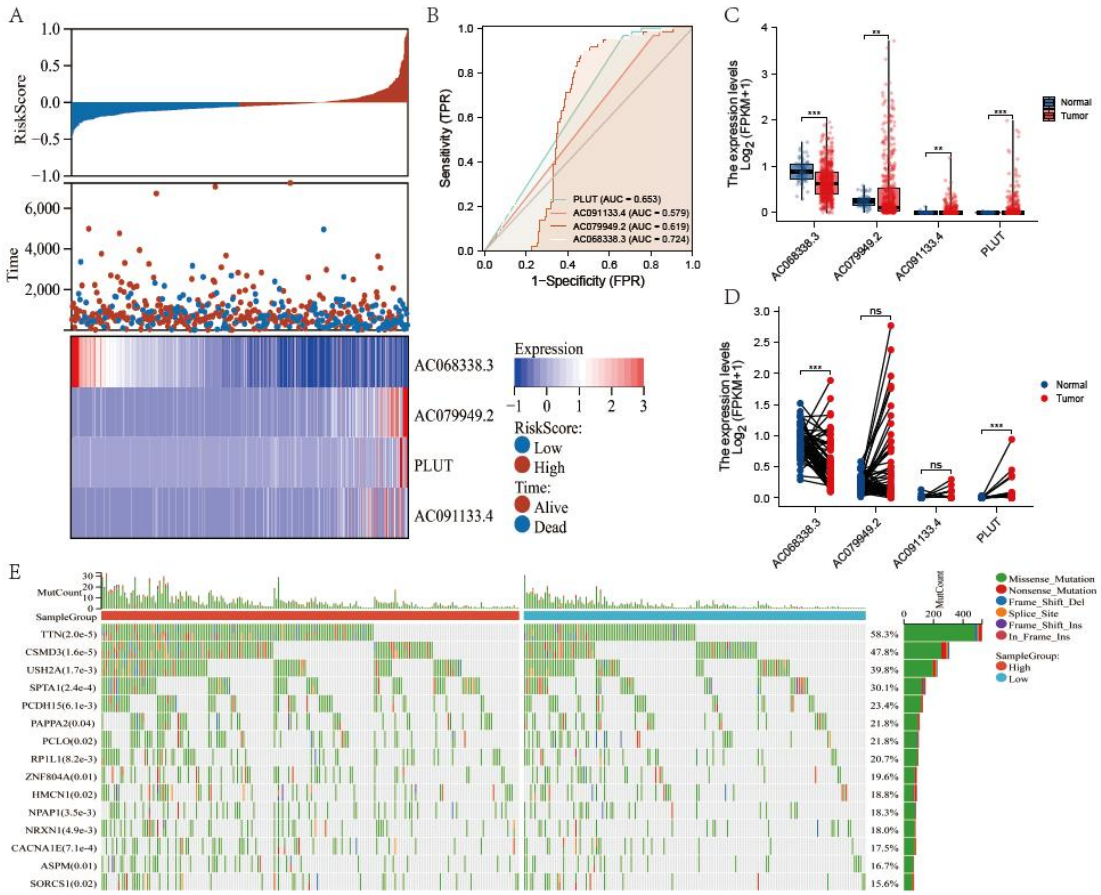

Fig. 5. Prognostic signature of the 4 RM-lncRNAs regulators in internal and external data set. (A) The distributions of prognostic signature- based risk scores， and heatmap of the expression of the 4regulators in different risk subgroups at the bottom (B) ROC curves of four RM-lncRNAs prognostic models to test 1-year, 3-year and 5-year performance of LUAD patients; (C-D) The boxplots show the significant expression differences between the unpaired and paired samples of the RM-lncRNAs prognostic model between normal samples and LUAD samples; (E) The incidence of somatic mutations in TCGA-LUAD was significantly different between the high and low risk groups in the prognostic RM-lncRNA model, and the mutation waterfall plot showed the genes with the highest mutation frequency in Top15.

3.4. Prognostic characteristics of clinical subgroups in a prognostic model of RM-lncRNAs

Box plots are used to show the prognostic models of RM-lncRNAs—PLUT, AC091133.4, AC079949.2, and AC068338.3 in TCGA-LUAD tumor samples, and the expression differences among different clinical variable subgroups, including Gender, Smoker, Pathologic stage, TNM, overall survival (OS), Disease-specific survival (DSS) and Primary therapy outcome. The results suggested that AC079949.2 was significantly overexpressed in Male (Fig. 6A), AC068338.3 was significantly underexpressed with smokers (Fig. 6B). PLUT, AC079949.2 were significantly overexpressed in Stage III&Stage IV and T3&T4 groups with advanced LUAD, while AC068338.3 was significantly underexpressed (Fig. 6C – F). High expression of AC091133.4 and low expression of AC068338.3 were significantly associated with shorter OS and DSS in LUAD (Fig. 6G,I). AC068338.3 was significantly underexpressed in LUAD patients of CR&PR (Fig. 6H).

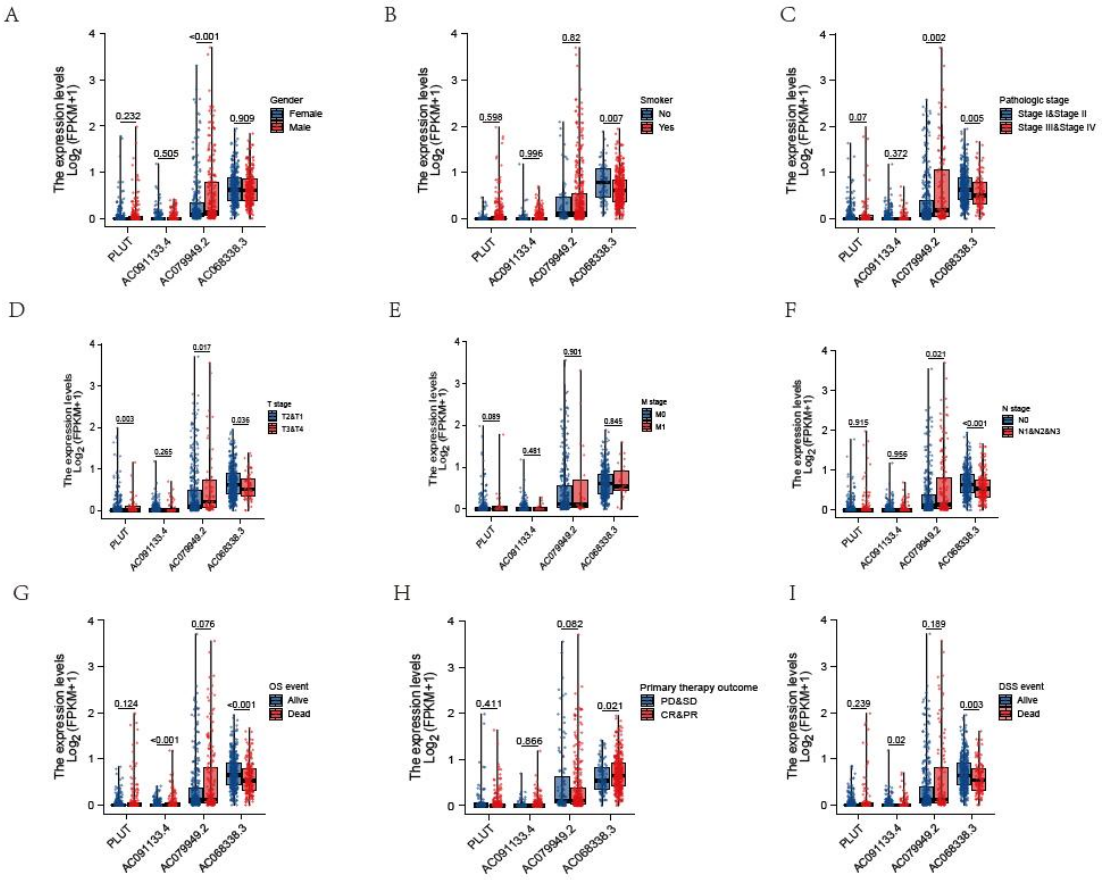

Fig. 6. Correlation analysis of clinical subgroups in RM-lncRNAs prognostic model. The differences in the expression of RM-lncRNAs prognostic model between different clinical variable subgroups in TCGA-LUAD tumor samples, including Gender (A), Smoker (B), Pathologic stage (C), TNM (D-F) , OS, DSS

and Primary therapy outcome (G-I).

3.5. OS prognostic analysis in LUAD

In order to further analyze the impact of the RM-lncRNAs prognostic model on LUAD more accurately, we used the OS time and survival status of the samples to describe the OS difference between the high and low expression group by drawing the K-M survival curve. We randomly divided the tumor samples from the TCGA-LUAD cohort into a training set and a validation set. Table 1 shows the baseline data of the clinical data of the patients between the two groups. The between-group variances were similar, and the data were normally distributed. Survival differences in the training group, test group, and overall TCGA-LUAD cohort, respectively. Consistent with the correlation of clinical syndrome differentiation, survival analysis found that PLUT (Fig. 7A–C), high expression of AC079949.2 (Fig. 7G–I), and low expression of AC068338.3 (Fig. 7D–F) were associated with a poor prognosis. OS status and shorter survival time were significantly correlated.Although there was no significant correlation with most clinical variables due to too few samples with AC091133.4 expression. The above analysis confirmed that the prognostic gene signature of RM-lncRNAs composed of 4 key lncRNAs we constructed was significantly associated with OS and tumor clinical variable subgroups in LUAD.

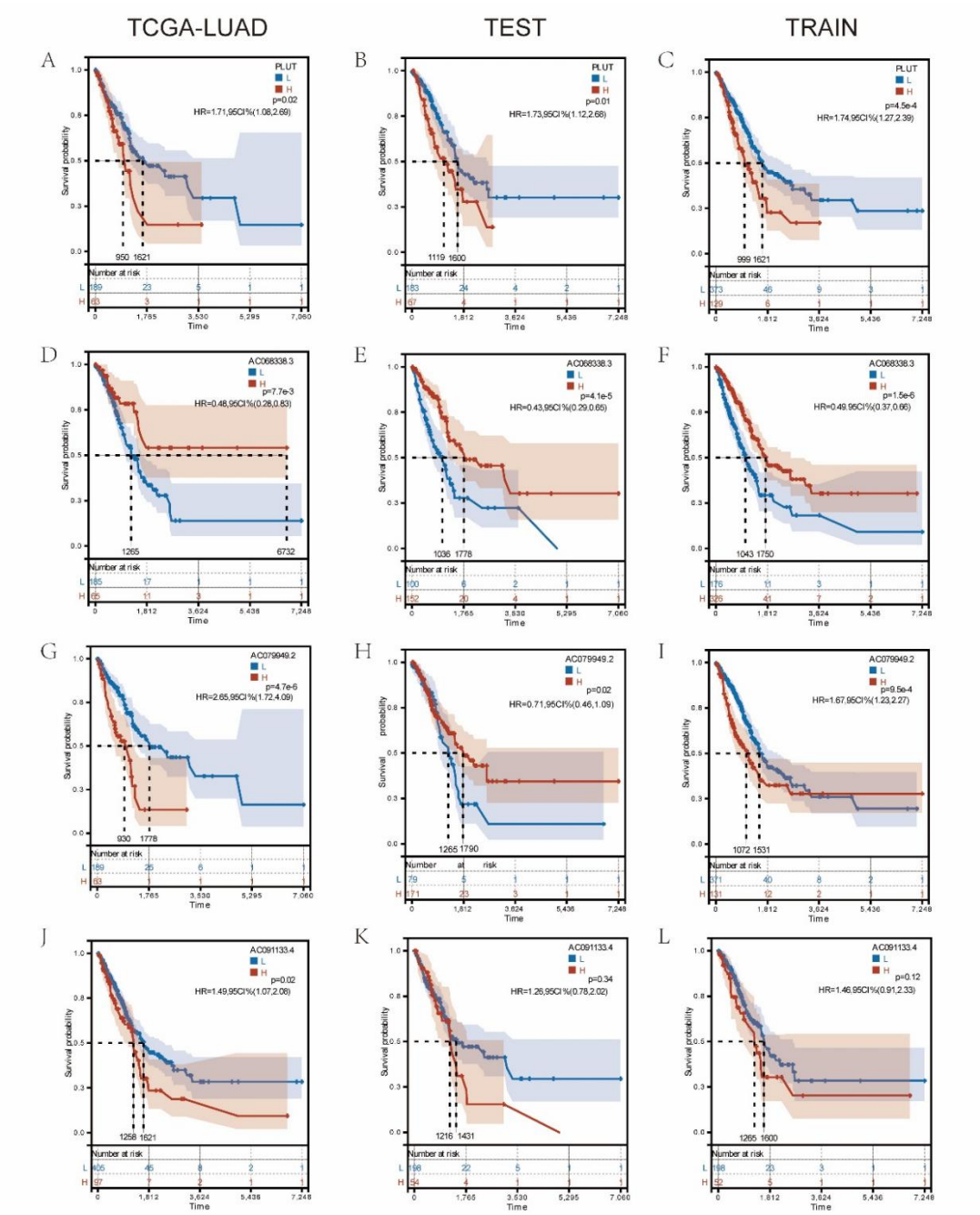

Fig. 7. OS prognostic analysis of RM-lncRNAs prognostic model in LUAD. (A-C) High expression of PLUT was significantly associated with poor KM OS prognosis in TCGA-LUAD cohort, training set and validation set, respectively; (D-F) Low expression of AC068338.3 in TCGA-LUAD cohort, training set and validation set, respectively was significantly associated with poor OS prognosis; (G-I) High expression of AC079949.2 was significantly associated with poor KM OS prognosis in the TCGA-LUAD cohort, training set and validation set, respectively.

Table 1 Clinical characteristics of LUAD patients in training and validation sets.

Characteristics	Train(N=256)	Test(N=257)	Total(N=513)	pvalue	FDR
Age					
Mean±SD	64.44±10.14	66.21±9.84	65.33±10.02		
Median[min-max]	65.00[38.00,87.00]	68.00[33.00,88.00]	66.00[33.00,88.00]		
Sex				0.23	0.71
FEMALE	144(28.07%)	130(25.34%)	274(53.41%)		
MALE	112(21.83%)	127(24.76%)	239(46.59%)		
Status				0.18	0.71
Alive	172(33.53%)	157(30.60%)	329(64.13%)		
Dead	84(16.37%)	100(19.49%)	184(35.87%)		
T				0.2	0.71
T1	78(15.20%)	94(18.32%)	172(33.53%)		
T2	140(27.29%)	134(26.12%)	274(53.41%)		
T3	23(4.48%)	22(4.29%)	45(8.77%)		
T4	12(2.34%)	7(1.36%)	19(3.70%)		
TX	3(0.58%)	0(0.0e+0%)	3(0.58%)		
N				0.44	0.71
N0	165(32.23%)	165(32.23%)	330(64.45%)		
N1	43(8.40%)	54(10.55%)	97(18.95%)		
N2	38(7.42%)	34(6.64%)	72(14.06%)		
N3	1(0.20%)	1(0.20%)	2(0.39%)		
NX	8(1.56%)	3(0.59%)	11(2.15%)		
M				0.07	0.42
M0	171(33.60%)	173(33.99%)	344(67.58%)		
M1	18(3.54%)	7(1.38%)	25(4.91%)		
MX	66(12.97%)	74(14.54%)	140(27.50%)		
Stge				0.09	0.44
Stge I	133(26.34%)	142(28.12%)	275(54.46%)		

Characteristics	Train(N=256)	Test(N=257)	Total(N=513)	pvalue	FDR
Stge II	57(11.29%)	65(12.87%)	122(24.16%)		
Stge III	43(8.51%)	39(7.72%)	82(16.24%)		
Stge IV	19(3.76%)	7(1.39%)	26(5.15%)		

3.6. Construction of PPI Molecular Interaction Network

The possible mechanisms of co-regulation, cooperation or competition between genes are important. In order to discover more relevant genes related to the Hub RM-lncRNA prognosis model, we constructed a network for the DEGs between high and low risk groups, and the limma algorithm obtained the 535 LUAD samples in the TCGA-LUAD dataset. 233 DEGs between high and low risk groups (|logFC| > 0.5, adj P-value < 0.05). A protein-protein interaction network (PPI) was constructed through the STRING database to reflect the intermolecular interactions, and the maximum confidence interaction score was set to 0.4, which was analyzed and visualized by Cytoscape's Network Analyzer tool (v3.7.2) (Fig. 8A). Top30 closely related genes were screened using the CytoHubba plugin (Fig. 8B). Meanwhile, the MCODE plugin screened and visualized 46 closely related genes of PPI network modules (Fig. 8C). We performed further gene enrichment analysis on the 30 intersection Hub genes obtained by the two clustering algorithms, including CDC20, UF2, UBE2C, TPX2, NCAPH, BUB1, AURKB, HJURP, NEK2, RRM2, NDC80, MELK, RACGAP1, TOP2A, TTK, CDCA5, BIRC5, AURKA, NUSAP1, PLK1, KIF2C, KIF4A, CCNB2, CENPA, NCAPG, PBK, CDK1, CCNB1, DLGAP5, CCNA2.

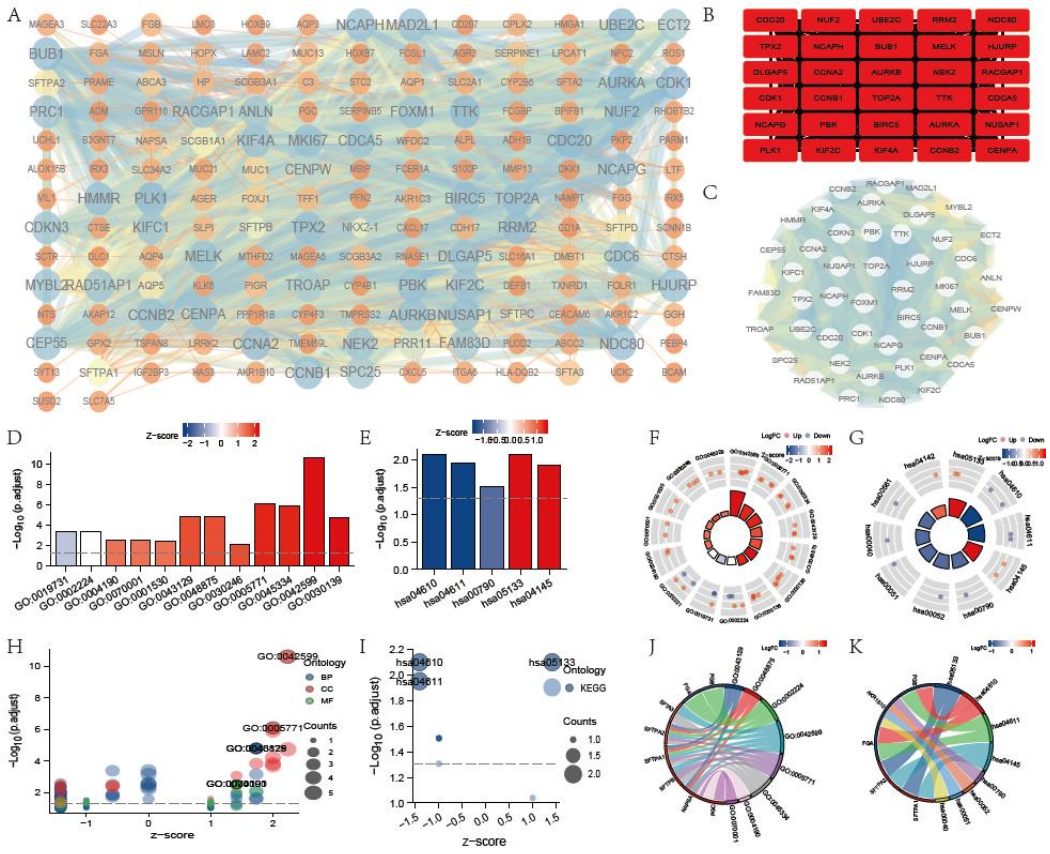

Fig. 8. Screening and functional enrichment of Hub DEGs between high and low risk groups in RM-lncRNAs prognostic model. (A) The network analyzer tool of Cytoscape (v3.7.2) visualized the PPI network of 223 DEGs (|LogFC| >0.5, adj P-value < 0.05) between the RM-lncRNAs prognostic model high and low risk groups in the TCGA-LUAD dataset, The maximum confidence interaction score is 0.4. As the degree of interaction increases, the color gradually changes from yellow to blue, and the font changes from small to large; (B) CytoHubba plugin is used to screen Top 30 closely related genes; (C) MCODE plugin filters and visualizes genes closely related to PPI network module; (D-K) Enrichment histogram, chord diagram, bubble diagram, and enrichment network diagram in turn of GO and KEGG pathway enrichment analysis based on 30 Hub DEGs.

3.7. Enrichment analysis of Hub genes associated with prognostic models of RM-lncRNAs

Next, we aimed to explore the underlying mechanisms by which the RM-lncRNAs prognostic model acts on LUAD. Through GO, KEGG enrichment analysis and to elucidate the Hub DEGs related to the RM-lncRNAs prognostic model, and analyze the possible enriched signaling pathways and molecular mechanisms. Enrichment results of GSEA may reveal the mechanism of action of the RM-lncRNAs prognostic

model in LUAD. GO enrichment analysis of the above-mentioned genes indicated that these Hub genes may exist in lamellar body, multivesicular body, clathrin-coated endocytic vesicle, etc., through surfactant homeostasis, chemical homeostasis within a tissue， Toll-like receptor signaling pathway and other pathways, and other functions (Fig. 8, Table 2–3).

Table 2 GO enrichment analysis of Top30 Hub DEGs with close relationship between high and low risk groups in RM-lncRNAs prognostic model.

Ontology	ID	Description	p.adjust	qvalue
BP	GO:0043129	surfactant homeostasis	1.54e-05	6.91e-06
BP	GO:0048875	chemical homeostasis within a tissue	1.54e-05	6.91e-06
BP	GO:0002224	toll-like receptor signaling pathway	3.94e-04	1.77e-04
CC	GO:0042599	lamellar body	2.38e-11	3.42e-12
CC	GO:0005771	multivesicular body	7.77e-07	1.11e-07
CC	GO:0045334	clathrin-coated endocytic vesicle	1.23e-06	1.76e-07
MF	GO:0004190	aspartic-type endopeptidase activity	0.003	0.001
MF	GO:0070001	aspartic-type peptidase activity	0.003	0.001

Table 3 KEGG enrichment analysis of Top30 Hub DEGs with close relationship between high and low risk groups in RM-lncRNAs prognostic model.

Ontology	ID	Description	p.adjust	qvalue
KEGG	hsa05133	Pertussis	0.008	8.41e-04
KEGG	hsa04610	Complement and coagulation	0.008	8.41e-04

Ontology	ID	Description	p.adjust	qvalue
		cascades		
KEGG	hsa04611	Platelet activation	0.011	0.001
KEGG	hsa04145	Phagosome	0.013	0.001
KEGG	hsa00790	Folate biosynthesis	0.031	0.003
KEGG	hsa00052	Galactose metabolism	0.031	0.003
KEGG	hsa00051	Fructose and mannose metabolism	0.031	0.003
KEGG	hsa00040	Pentose and glucuronate interconversions	0.031	0.003

Subsequently, GSEA based on the RM-lncRNAs prognostic model. Implications for high-risk groups identified by the RM-lncRNA prognostic model were associated with DNA damage and repair, cell cycle, aerobic glycolysis and gluconeogenesis, pyrimidine metabolism, proteasomal degradation, hematoxylation of important proteins, and the development of various cancers and pathways were closely related (Fig. 9, Table 4). In this 4 lncRNA prognostic gene signature, only AC068338.3 is a potential protective factor, while PLUT, AC091133.4, and AC079949.2 are all potential risk indicators.

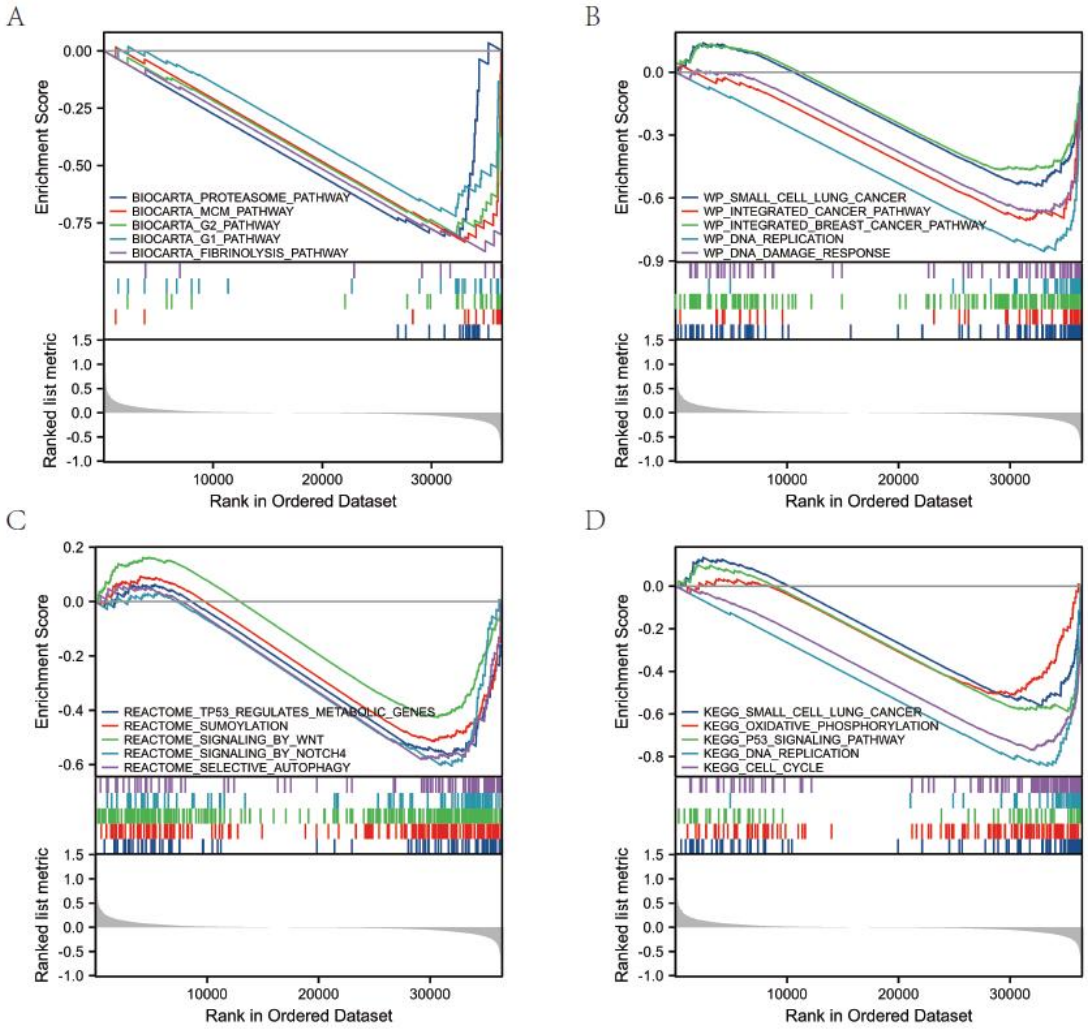

Fig. 9. Gene Set Enrichment Analysis (GSEA) between high and low risk groups in the RM-lncRNAs prognostic model. (A) High risk group is enriched in WP database and enriched in SMALL CELL LUNG CANCER, INTEGRATED CANCER PATHWAY, INTEGRATED BREAST CANCER PATHWAY, DNA REPLICATION, DNA DAMAGE RESPONSE; (B) High risk group is enriched in REACTOME database and enriched in TP53 REGULATES METABOLIC GENES, SUMOYLATION, SIGNALING BY WNT, SIGNALING BY NOTCH4, SELECTIVE AUTOPHAGY; (C) High-risk groups are enriched in KEGG database in SMALL CELL LUNG CANCER, KEGG OXIDATIVE PHOSPHORYLATION, P53 SIGNALING PATHWAY, DNA REPLICATION, CELL CYCLE; (D) The high-risk group was enriched in the BIOCARTA database enriched in PROTEASOME PATHWAY, BIOCARTA MCM PATHWAY, G2 PATHWAY, G1 PATHWAY, FIBRINOLYSIS PATHWAY.

Table 4 Gene Set Enrichment Analysis (GSEA) between high and low risk groups in the RM-lncRNAs prognostic model.

ID	ES	NES	p.adjust	q
KEGG_CELL_CYCLE	-0.76956	-2.25126	0.02513	0.020536
KEGG_DNA_REPLICATION	-0.8452	-2.0946	0.02513	0.020536
KEGG_PROTEASOME	-0.84283	-2.15983	0.02513	0.020536
PID_ATR_PATHWAY	-0.82902	-2.07439	0.02513	0.020536
PID_AURORA_B_PATHWAY	-0.85249	-2.12458	0.02513	0.020536
PID_PLK1_PATHWAY	-0.83972	-2.15186	0.02513	0.020536
REACTOME_ACTIVATION_OF_ATR_IN_RESPONSE_TO_REPLICATION_STRESS	-0.85287	-2.12287	0.02513	0.020536
REACTOME_ACTIVATION_OF_THE_PRE_REPLICATIVE_COMPLEX	-0.88645	-2.15381	0.02513	0.020536
REACTOME_APC_C_CDH1_MEDIATED_DEGRADATION_OF_CDC20_AND_OTHER_APC_C_CDH1_TARGETED_PROTEINS_IN_LATE_MITOSIS_EARLY_G1	-0.7854	-2.15424	0.02513	0.020536
REACTOME_APC_C_MEDIATED_DEGRADATION_OF_CELL_CYCLE_PROTEINS	-0.80713	-2.28936	0.02513	0.020536
REACTOME_ASSEMBLY_OF_THE_PRE_REPLICATIVE_COMPLEX	-0.84521	-2.297	0.02513	0.020536
REACTOME_AUF1_HNRNP_D0_BINDS_AND_DESTABILIZES_MRNA	-0.78595	-2.07664	0.02513	0.020536
REACTOME_CELL_CYCLE_CHECKPOINTS	-0.79036	-2.49464	0.02513	0.020536
REACTOME_CELL_CYCLE_MITOTIC	-0.72518	-2.42103	0.02513	0.020536
REACTOME_CHROMOSOME_MAINTE	-0.74138	-2.11174	0.02513	0.020536

ID	ES	NES	p.adjust	q
NANCE				
REACTOME_DEGRADATION_OF_DVL	-0.76046	-2.0232	0.02513	0.020536
REACTOME_DEGRADATION_OF_GLI1_				
BY_THE_PROTEASOME	-0.76092	-2.03951	0.02513	0.020536
REACTOME_DNA_DOUBLE_STRAND_				
BREAK_REPAIR	-0.68357	-2.01293	0.02513	0.020536
REACTOME_DNA_REPLICATION	-0.82154	-2.40773	0.02513	0.020536
REACTOME_DNA_REPLICATION_PRE_				
INITIATION	-0.85136	-2.40258	0.02513	0.020536
REACTOME_DNA_STRAND_ELONGATI				
ON	-0.86377	-2.08591	0.02513	0.020536
REACTOME_G1_S_DNA_DAMAGE_CH				
ECKPOINTS	-0.75883	-2.06225	0.02513	0.020536
REACTOME_G1_S_SPECIFIC_TRANSCR				
IPTION	-0.86573	-2.04288	0.02513	0.020536
REACTOME_G2_M_CHECKPOINTS	-0.81999	-2.42426	0.02513	0.020536
REACTOME_G2_M_DNA_DAMAGE_CH				
ECKPOINT	-0.78157	-2.09528	0.02513	0.020536
REACTOME_HOMOLOGOUS_DNA_PAI				
RING_AND_STRAND_EXCHANGE	-0.79078	-2.00439	0.02513	0.020536
REACTOME_HOMOLOGY_DIRECTED_				
REPAIR	-0.71815	-2.06956	0.02513	0.020536
REACTOME_HOST_INTERACTIONS_OF				
_HIV_FACTORS	-0.68882	-2.02021	0.02513	0.020536
REACTOME_M_PHASE	-0.70037	-2.27782	0.02513	0.020536
REACTOME_METABOLISM_OF_POLYA				
MINES	-0.75184	-2.00857	0.02513	0.020536
REACTOME_MITOTIC_G1_PHASE_AND	-0.7835	-2.34322	0.02513	0.020536

ID	ES	NES	p.adjust	q
_G1_S_TRANSITION				
REACTOME_MITOTIC_G2_G2_M_PHAS				
ES	-0.69885	-2.16578	0.02513	0.020536
REACTOME_MITOTIC_METAPHASE_A				
ND_ANAPHASE	-0.7699	-2.42722	0.02513	0.020536
REACTOME_MITOTIC_PROMETAPHAS				
E	-0.72209	-2.24396	0.02513	0.020536
REACTOME_MITOTIC_SPINDLE_CHEC				
KPOINT	-0.78094	-2.27118	0.02513	0.020536
REACTOME_NEGATIVE_REGULATION				
_OF_NOTCH4_SIGNALING	-0.77381	-2.04113	0.02513	0.020536
REACTOME_ORC1_REMOVAL_FROM_				
CHROMATIN	-0.83795	-2.27979	0.02513	0.020536
REACTOME_PROCESSING_OF_DNA_D				
OUBLE_STRAND_BREAK_ENDS	-0.7495	-2.03058	0.02513	0.020536
REACTOME_REGULATION_OF_RUNX2				
_EXPRESSION_AND_ACTIVITY	-0.75843	-2.07441	0.02513	0.020536
REACTOME_RESOLUTION_OF_SISTER				
_CHROMATID_COHESION	-0.79703	-2.32966	0.02513	0.020536
REACTOME_RHO_GTPASES_ACTIVAT				
E_FORMINS	-0.75563	-2.2465	0.02513	0.020536
REACTOME_S_PHASE	-0.76316	-2.31135	0.02513	0.020536
REACTOME_SCF_SKP2_MEDIATED_DE				
GRADATION_OF_P27_P21	-0.76166	-2.04149	0.02513	0.020536
REACTOME_SEPARATION_OF_SISTER				
_CHROMATIDS	-0.77814	-2.40389	0.02513	0.020536
REACTOME_STABILIZATION_OF_P53	-0.76936	-2.0469	0.02513	0.020536
REACTOME_SURFACTANT_METABOLI	0.883621	2.039876	0.02513	0.020536

ID	ES	NES	p.adjust	q
SM				
REACTOME_SWITCHING_OF_ORIGINS				
_TO_A_POST_REPLICATIVE_STATE	-0.80286	-2.27702	0.02513	0.020536
REACTOME_THE_ROLE_OF_GTSE1_IN				
_G2_M_PROGRESSION_AFTER_G2_CH				
ECKPOINT	-0.79793	-2.21032	0.02513	0.020536
WP_CELL_CYCLE	-0.76823	-2.24497	0.02513	0.020536
WP_DNA_IRDAMAGE_AND_CELLULA				
R_RESPONSE_VIA_ATR	-0.73601	-2.04605	0.02513	0.020536
WP_DNA_REPLICATION	-0.85596	-2.1696	0.02513	0.020536
WP_G1_TO_S_CELL_CYCLE_CONTROL	-0.74342	-2.01411	0.02513	0.020536
WP_GASTRIC_CANCER_NETWORK_1	-0.87993	-2.04436	0.02513	0.020536
WP_PARKINUBIQUITIN_PROTEASOMA				
L_SYSTEM_PATHWAY	-0.74061	-2.01102	0.02513	0.020536
WP_RETINOBLASTOMA_GENE_IN_CA				
NCER	-0.80406	-2.26576	0.02513	0.020536

3.8. Validation of clinical significance and predictive accuracy of prognostic gene signatures of RM-lncRNAs

In this part, we combined clinical features and risk characteristics to verify the reliability of this prognostic RM-lncRNAs gene signature. A nomogram map containing important clinical variable parameters affecting survival in LUAD and its calibration plot were created, showing the results of multivariate Cox regression analysis. The effectiveness of age, sex, tumor TNM stage and clinical grade, and risk scores of RM-lncRNAs gene signatures in predicting 1-, 3-, and 5-year survival in LUAD was assessed (Fig. 10A－B). For the results to show that the risk score as a predictor has a better and more significant predictive value than other clinical features. Significant significance for LUAD OS included prognostic RM-lncRNAs gene

signature risk score, tumor T stage and N stage.

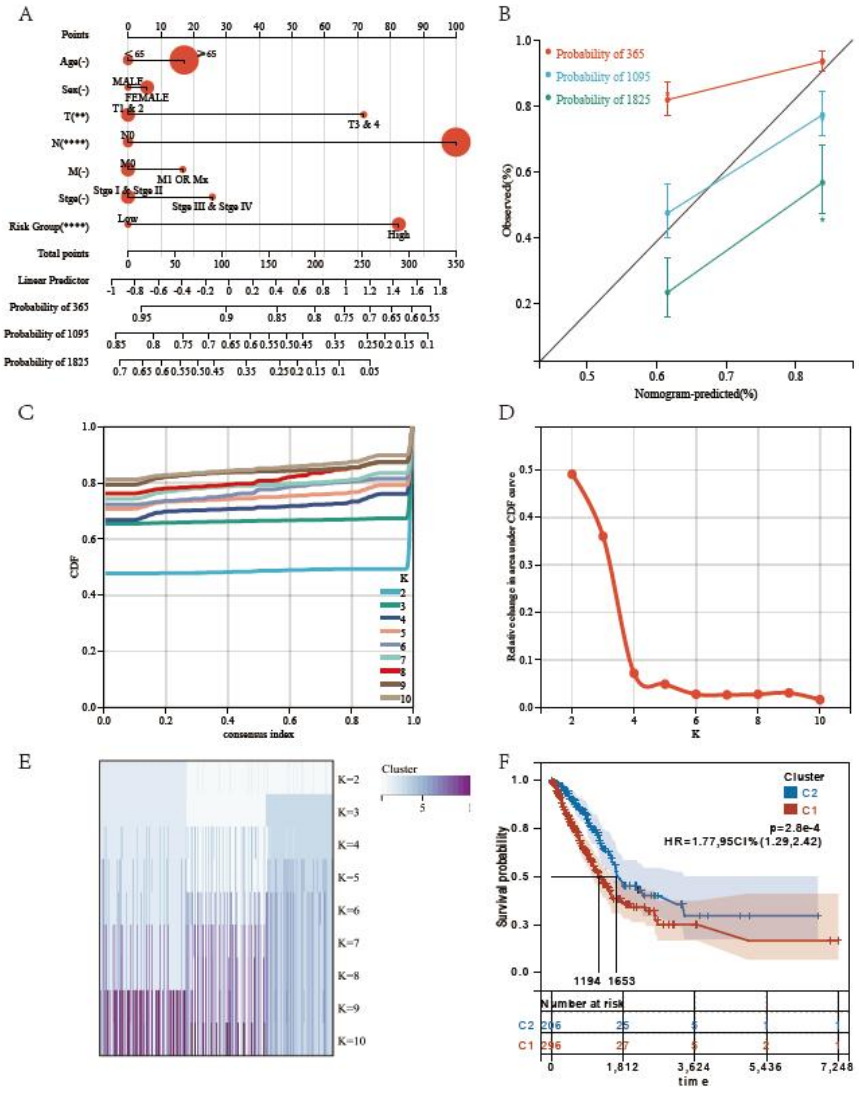

Fig. 10. Consistent clustering of prognostic RM-lncRNAs gene signatures. (A-B) Nomogram and calibration curves were evaluated for the effectiveness of risk scores based on age, sex, tumor TNM stage and clinical grade, and genetic signatures of RM-lncRNAs in predicting 1-/3-/5-year survival in LUAD; (C) Consensus clustering diagram based on prognostic RM-lncRNAs gene signature; (D) When K = 2, secondary consensus clustering of LUAD samples is better significant; (E) Consensus clustering sample distribution diagram ; (F) Survival differences between groups based on molecular subtype Cluster1 & 2 mediated by gene signatures of RM-lncRNAs.

Table 5 Correlation of prognostic gene signatures of RM-lncRNAs with immune cell infiltration in LUAD-TMB.

RM-lncRNAs	Immune cells	Cor	p.adjust
AC068338.3	NK CD56dim cells	-0.11177	0.009672
	CD8 T cells	0.129982	0.002593
	pDC	0.132001	0.002217
	NK cells	0.145736	0.000722
	Mast cells	0.14904	0.000543
	T helper cells	-0.15578	0.000298
	Th17 cells	0.157613	0.000252
	TFH	0.162308	0.000163
	Eosinophils	0.16647	0.00011
	Tgd	-0.18575	1.53E-05
	NK CD56bright cells	0.248446	5.72E-09
	Th2 cells	-0.40265	2.86E-22
AC079949.2	B cells	-0.11706	0.006718
	Cytotoxic cells	-0.12607	0.00349
	Eosinophils	-0.13677	0.001519
	Th1 cells	-0.13934	0.001232
	T cells	-0.14723	0.000635
	pDC	-0.15788	0.000246
	Mast cells	-0.16537	0.000122
	Th17 cells	-0.16565	0.000119
	Macrophages	-0.16617	0.000113
	Th2 cells	0.193414	6.61E-06
	DC	-0.19664	4.59E-06
	iDC	-0.20767	1.26E-06
	Tgd	0.276338	7.83E-11
	TFH	-0.28483	1.92E-11

RM-lncRNAs	Immune cells	Cor	p.adjust
AC091133.4	Neutrophils	-0.10407	0.016038
	iDC	-0.10574	0.014412
	Eosinophils	-0.10791	0.012513
	Tcm	-0.13033	0.002524
	Mast cells	-0.21361	6.13E-07
PLUT	Tem	-0.10539	0.014734
	T cells	-0.1154	0.00754
	Th2 cells	0.115779	0.007346
	NK cells	-0.124	0.004072
	Cytotoxic cells	-0.12743	0.003151
	pDC	-0.12764	0.003102
	DC	-0.13859	0.001311
	Th1 cells	-0.15709	0.000265
	TFH	-0.16316	0.00015
	iDC	-0.17087	7.12E-05
	Macrophages	-0.18816	1.18E-05

3.9. Consistent clustering of gene signatures of prognostic RM-lncRNAs

The above analysis proves that our constructed RM-lncRNAs gene signature can well predict the OS and clinical prognosis of LUAD. We performed unsupervised clustering of 503 LUAD samples based on the molecular subtypes mediated by the gene signatures of the four RM-lncRNAs.Grouped with Cluster1 (n = 296) and Cluster2 (n = 207) reflected that K = 2 was the best number of clusters with the highest intra-group correlation and minimal inter-group interference (Fig. 10C – E). Therefore, LUAD patients were divided into two subgroups. Subsequently, we evaluated the survival difference between the Cluster1 & 2 groups, and the KM survival analysis showed that the Cluster2 patients had a significant survival advantage, p=2.8e-4, HR=1.77 (1.29-2.42) (Fig. 10F).

3.10. Characteristics of the immune microenvironment in a prognostic model of RM-lncRNAs

Furthermore, we found that the features of 4 lncRNA prognostic gene signatures were correlated with TME and expression of key immune checkpoints. Based on the above data, we separately analyzed the differences in TME immune cell infiltration between the high- and low-risk subgroups, as well as the RM-lncRNAs prognostic model consistent clustering Cluster1 & 2 groups, and displayed them as box plots. The results of CIBERSORT showed differences in the distribution of 22 immune infiltrating cells between the high and low risk groups of the RM-lncRNAs prognostic model (Fig. 11A), and between the RM-lncRNAs prognostic model consistent clustering groups (Fig. 11B). The results showed that B cells memory, T cells CD4 memory resting, Macrophages M1, Mast cells resting, and Dendritic cells resting in the high-risk group of the RM-lncRNAs prognostic model and in the consistent cluster Cluster1 were significantly underexpressed between the two types of groups. In addition, the high-risk group also had significantly less infiltration of Monocytes, T cells CD4 memory activated, and Cluster1 had significantly less infiltration of T cells regulatory (Tregs), NK cells resting, Macrophages M0, and Mast cells activated (Fig. 11A – B). Combined with the effect of immune cell infiltration on tumor tissue, the results suggest that the prediction of poor risk prognosis by 4 lncRNA prognostic gene signature is also closely related to TMB in LUAD tissue. Consistent cluster grouping based on this prognostic model can well distinguish the immune infiltrating morphology of poor LUAD. Cluster 2 is considered to be a "hot tumor" with a better prognosis, while cluster 1 is considered a "cold tumor" with a poor prognosis.

In addition, based on the high- and low-risk grouping and consistent clustering of the RM-lncRNAs prognostic model, we analyzed the significant differences in the stromal score and immune score between the risk groups of the LUAD samples, and the low risk was significantly higher (Fig. 11C – E). Consistent clustering of ESTIMATE scores and stromal scores for Cluster 2 (Fig. 11F – H). It was also

consistent with the immune infiltration distribution results, supporting the reliability of the prognostic model of RM-lncRNAs.

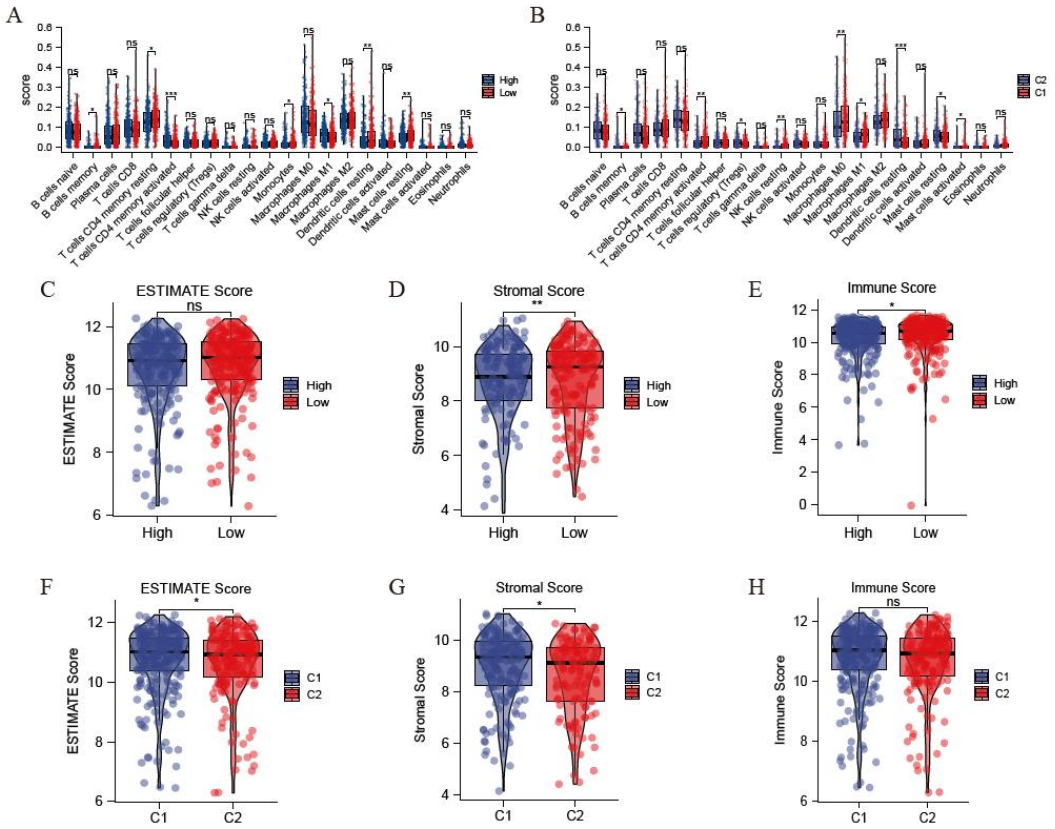

Fig. 11. Differences in immune infiltration in prognostic models of RM-lncRNAs. (A) Box plot of differences in TME immune cell infiltration between high and low risk subgroups of RM-lncRNAs prognostic model ;(B) Consistent clustering of cluster 1 & 2 of differences in TME immune cell infiltration box plot; (C-E) RM-lncRNAs prognostic model of high and low The difference box group comparison chart of ESTIMATEScore, ImmuneScore and StromalScore of risk subgroups; (F-H) Box plots comparison chart of ESTIMATEScore, ImmuneScore and StromalScore of RM-lncRNAs prognostic model consistent clustering group Cluster1 & 2.

3.11. Correlation of immune infiltrating cells

Furthermore, we sought to determine the correlation between molecular expression subsets and immune-infiltrating cells of the RM-lncRNAs prognostic model. We reflect the correlation between the 4 lncRNA prognostic gene signatures and immune cell infiltration by lollipop plots, respectively. Fig. 12A – D shows the correlation

analysis of immune infiltrating cells of AC079949.2, AC091133.4, AC068338.3, and PLUT, respectively. result. In order to reflect whether the 4 lncRNA prognostic gene signatures are differentially correlated with LUAD, we analyzed the effect of the expression levels of RM-lncRNAs prognostic model on the differences in immune cell infiltration in LUAD based on the TCGA-LUAD database. Considering the insufficient amount of gene expression samples, we only showed the differences in immune cell infiltration between AC079949.2, AC068338.3 high and low expression groups, and the results suggested that immune cells such as TBNK had significant infiltration differences (Fig. 12E–F). At the same time, a scatterplot with a strong correlation (|Cor|>0.2) is shown (Fig. 12G–K).

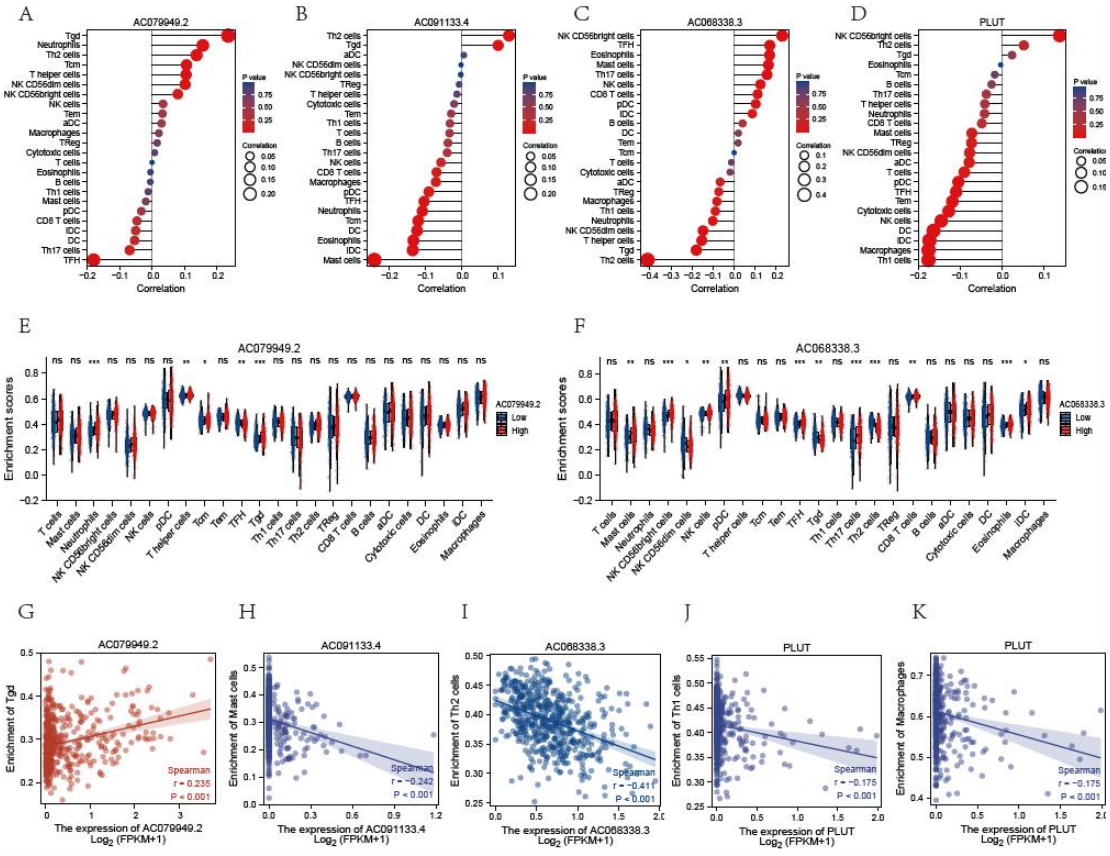

Fig. 12. Correlation of immune infiltrating cells. (A-D) Lollipop plot of correlation between 4 lncRNA prognostic gene signature and immune cell infiltration; (E-F) Differential box type of immune cell infiltration between AC079949.2, AC068338.3 high- and low- expression groups in TCGA-LUAD Group comparison plots; (G-K) Scatter plots showing the correlation between the RM-lncRNAs prognostic model and significantly correlated immune cells in LUAD.

4. Discussion

LUAD is a major cause of tumor-related death, and its tumorigenesis involves the accumulation of genetic and epigenetic events in respiratory epithelial cells [51,52], as well as antitumor immune responses [53]. Reversible dynamic RM, as a major chemical modification type, is involved in important tumor malignant phenotypes, and regulates the body's metabolism and fate [53,54] As epitranscriptomic-driven development unfolds, poor prognosis due to inefficiency of treatment and failure of early diagnosis is still commonplace today [55,56]. RNA modification is involved in the occurrence and progression of lung cancer by reducing the stability or expression of mRNA [57], encoding the suppressor of oncogenes to reduce its inhibitory effect and enhance the stability and expression of pro-oncogene transcripts [58]. However, whether m6A-/m1A-/m5C/-m7G-related regulators are involved in the development of LUAD and TME immune cells through their effects on lncRNAs. Little progress has been made in the study of infiltration [59]. There is evidence for an interaction between lncRNAs and RM in tumors. Although there are currently many biological markers for predicting prognosis in LUAD, unfortunately, there are few studies on lncRNAs [58–60]. In this study, for the first time, we identified 210 RM-related lncRNAs that were significantly differentially expressed in tumor tissues in TCGA-LUADt, of which 45 RM-lncRNAs were confirmed to have prognostic value. The prognostic significance of the RM-lncRNAs gene signature was further validated by Cox regression combining clinical and risk characteristics. All results supported the clinical significance of the RM-lncRNAs gene signature (PLUT, AC091133.4, AC068338.3 and AC079949.2) as a poor prognosis in LUAD.

A genome-wide DNA methylation analysis of early stage I LUAD has confirmed that abnormal methylation of the PLUT promoter can predict the risk of early recurrence in patients with early stage I adenocarcinoma [61,62]. Aberrant methylation of PDX1 is mainly through the transcriptional regulation of PLUT, thereby mediating the occurrence of lung adenocarcinoma. AC068338.3 had been reported to act as an immune-related lncRNA that plays a crucial role in the tumor immune

microenvironment of LUAD and is associated with the progression of LUAD tumorigenesis [62,63]. There were many related reports on AC079949.2, for example, it is related to the OS of ESCA patients, and in LUAD, it can be used as an immune- and hypoxia-related lncRNA to predict the clinical stratification of patients, so as to judge the prognosis and immune microenvironment of patients [64,65]. Although there is no report on AC091133.4, the findings of this study have drawn attention to the impact of this molecule on the prognosis of patients with LUAD.

Therefore, we further grouped 2 clusters by consensus clustering analysis based on the RM-lncRNAs gene signature in LUAD. The differences in immune cell infiltration of TMB in LUAD tissues were also analyzed. The results showed that cluster 1 had better OS than cluster 2. A relationship between RM-related lncRNAs and poor prognosis in LUAD was supported.

Based on the above findings, we further compared the the difference of immune microenvironmental landscape of each LUAD sample between risk groups and the clustering based on the RM-lncRNAs gene signature, TME and immune examinations relationship between points. Cluster 1 and low-risk groups were enriched with a large number of immune-infiltrating cells, including important tertiary lymphoid structures such as TBNK cells. Regardless of the effect of 4 RM-lncRNAs on the OS of LUAD in the training set or test set of TCGA-LUAD, the results suggested that AC068338.3 is a potential protective factor, while PLUT, AC091133.4, and AC079949.2 are all potential risk indicators. Consistent with the survival analysis results of risk groups bassed on 4 RM-lncRNA gene signatures. All the results support that our RM-lncRNAs prognostic model can effectively predict the overall survival of LUAD patients in different clinical subgroups, and at the same time infer immunotherapy efficacy by predicting differences in immune microenvironment infiltration. We also validated the predictive ability of the prognostic model for patients with poor clinical outcomes and immune response tolerance in high-risk populations. The prognostic models of RM-related lncRNAs are highly heterogeneous among different risk groups. Next, we investigated the incidence of my somatic mutation between high- and low-risk group in TCGA-LUAD RM-lncRNA model Top15 genes including N1,

NPAP1, NRXN1, CACNA1E, ASPM, SORCS1. Notably, we providing a potential novel direction for the treatment of LUAD. We tried to explore the construction and validation of a new LUAD prognostic model based on m6A-/m1A-/m5C-/m7G-related regulatory factors, and verified that the prognostic model can be used as an independent factor to affect the occurrence and development of LUAD. Results of our RM-lncRNAs prognostic model are helpful for clinical diagnosis and treatment according to the pathological stage of LUAD. Meanwhile, more targeted immunotherapy related to RM-lncRNAs in the future opens up new possibilities.

5. Conclusion

Our study initially used Cox regression analysis to screen out 4 m6A-/m1A-/m5C-/m7G-RM related genes (TRDMT1, IGF2BP3, HNRNPC, IGF2BP1) associated with the OS rates of LUAD. The 210 m6A-/m1A-/m5C-/m7G-related lncRNAs with which they were significantly co-expressed were performed to construct a prognostic model using the least absolute shrinkage method and selection operator. Four key prognostic RM-lncRNAs signatures were significantly associated with OS in LUAD patients. At the same time, nomogram was established to analyze the important clinical variables and OS of LUAD within 1, 3 and 5 years, and the reliability was verified by calibration curve and subgroup KM survival analysis. Through cluster analysis, the m6A-/m1A-/m5C-/m7G-related lncRNAs in the TCGA -LUAD database were divided into two clusters. Finally, variable subgroup differences in immune cell infiltration were analyzed. Thus, the predictive significance of the risk model of RM regulators for the clinical prognosis of LUAD was verified. The above comprehensive data support that the four m1A-, m5C-, m6A-, and m7G-related regulatory factors we constructed may be promising biomarkers for future research.

References

[1] Schosserer M, Minois N, Angerer TB, Amring M, Dellago H, Harreither E, et al. Methylation

of ribosomal RNA by NSUN5 is a conserved mechanism modulating. Nat Commun. 6 (2015) 6158, https://doi.org/10.1038/ncomms7158.
[2] Li X, Xiong X, Wang K, Wang L, Shu X, Ma S, et al. Transcriptome-wide mapping reveals reversible and dynamic N(1)-methyladenosine. Nat Chem Biol. 12 (5) (2016) 311–316, https://doi.org/10.1038/nchembio.2040.
[3] He M, Wu G, Wang Z, Ren K, Yang Z, Xue Q. Development and validation of a TRP-related gene signature for overall survival prediction in lung adenocarcinoma. Frontiers in Genetics. 13 (2022) 905650, https://doi.org/10.3389/fgene.2022.905650.
[4] Zhou W, Wang X, Chang J, Cheng C, Miao C. The molecular structure and biological functions of RNA methylation, with special emphasis on the roles of RNA methylation in autoimmune diseases. Crit Rev Clin Lab Sci. 59 (3) (2022) 203–218, https://doi.org/10.1080/10408363.2021.2002256.
[5] Chai RC, Wu F, Wang QX, Zhang S, Zhang KN, Liu YQ, et al. m^{6}A RNA methylation regulators contribute to malignant progression and have clinical prognostic impact in gliomas. Aging (Albany NY). 11 (4) (2019) 1204–1225, https://doi.org/10.18632/aging.101829.
[6] Li F, Yi Y, Miao Y, Long W, Long T, Chen S, et al. N^6-Methyladenosine Modulates Nonsense-Mediated mRNA Decay in Human Glioblastoma. Cancer Res. 79 (22) (2019) 5785–5798, https://doi.org/10.1158/0008-5472.CAN-18-2868.
[7] Cheng Y, Luo H, Izzo F, Pickering BF, Nguyen D, Myers R, et al. m^{6}A RNA Methylation Maintains Hematopoietic Stem Cell Identity and Symmetric Commitment. Cell Rep. 28 (7) (2019) 1703–1716.e6, https://doi.org/10.1016/j.celrep.2019.07.032.
[8] Cui YH, Yang S, Wei J, Shea CR, Zhong W, Wang F, et al. Autophagy of the m^{6}A mRNA demethylase FTO is impaired by low-level arsenic exposure to promote tumorigenesis. Nat Commun. 12 (1) (2021) 2183, https://doi.org/10.1038/s41467-021-22469-6.
[9] Spitale RC, Flynn RA, Zhang QC, Crisalli P, Lee B, Jung JW, et al. Structural imprints in vivo decode RNA regulatory mechanisms. Nature. 519 (7544) (2015) 486–490, https://doi.org/10.1038/nature14263.
[10] Li Y, Xiao J, Bai J, Tian Y, Qu Y, Chen X, et al. Molecular characterization and clinical relevance of m^{6}A regulators across 33 cancer types. Mol Cancer. 18 (1) (2019) 137, https://doi.org/10.1186/s12943-019-1066-3.
[11] Liu ZX, Li LM, Sun HL, Liu SM. Link Between m6A Modification and Cancers. Front Bioeng Biotechnol. 6 (2018) 89, https://doi.org/10.3389/fbioe.2018.00089.
[12] Zhang C, Jia G. Reversible RNA Modification N^1-methyladenosine (m^{1}A) in mRNA and tRNA. Genomics Proteomics Bioinformatics. 16 (3) (2018) 155–161, https://doi.org/10.1016/j.gpb.2018.03.003.
[13] Bar-Yaacov D, Frumkin I, Yashiro Y, Chujo T, Ishigami Y, Chemla Y, et al. Mitochondrial 16S rRNA Is Methylated by tRNA Methyltransferase TRMT61B in All Vertebrates. PLoS Biol. 14 (9) (2016) e1002557, https://doi.org/10.1371/journal.pbio.1002557.
[14] Chen X, Li A, Sun BF, Yang Y, Han YN, Yuan X, et al. 5-methylcytosine promotes pathogenesis of bladder cancer through stabilizing mRNAs. Nat Cell Biol. 21 (8) (2019) 978–990, https://doi.org/10.1038/s41556-019-0361-y.
[15] Ramanathan A, Robb GB, Chan SH. mRNA capping: biological functions and applications. Nucleic Acids Res. 44 (16) (2016) 7511–7526, https://doi.org/10.1093/nar/gkw551.
[16] Pandolfini L, Barbieri I, Bannister AJ, Hendrick A, Andrews B, Webster N, et al. METTL1

Promotes let-7 MicroRNA Processing via m7G Methylation. Mol Cell. 74 (6) (2019) 1278–1290.e9, https://doi.org/10.1016/j.molcel.2019.03.040.
[17] Teng PC, Liang Y, Yarmishyn AA, Hsiao YJ, Lin TY, Lin TW, et al. RNA Modifications and Epigenetics in Modulation of Lung Cancer and Pulmonary Diseases. Int J Mol Sci. 22 (19) (2021) 10592, https://doi.org/10.3390/ijms221910592.
[18] Schwartz S, Agarwala SD, Mumbach MR, Jovanovic M, Mertins P, Shishkin A, et al. High-resolution mapping reveals a conserved, widespread, dynamic mRNA methylation program in yeast meiosis. Cell. 155 (6) (2013) 1409–1421, https://doi.org/10.1016/j.cell.2013.10.047.
[19] Salditt-Georgieff M, Jelinek W, Darnell JE, Furuichi Y, Morgan M, Shatkin A. Methyl labeling of HeLa cell hnRNA: a comparison with mRNA. Cell. 7 (2) (1976) 227–237, https://doi.org/10.1016/0092-8674(76)90022-2.
[20] Wu XR, Chen Z, Liu Y, Chen ZZ, Tang F, Chen ZZ, et al. Prognostic signature and immune efficacy of m^1 A-, m^5 C- and m^6 A-related regulators in cutaneous melanoma. J Cell Mol Med. 25 (17) (2021) 8405–8418, https://doi.org/10.1111/jcmm.16800.
[21] Xu L, Zhang C, Yin H, Gong S, Wu N, Ren Z, et al. RNA modifications act as regulators of cell death. RNA Biol. 18 (12) (2021) 2183–2193, https://doi.org/10.1080/15476286.2021.1925460.
[22] Song H, Li H, Ding X, Li M, Shen H, Li Y, et al. Long non-coding RNA FEZF1-AS1 facilitates non-small cell lung cancer progression via the ITGA11/miR-516b-5p axis. Int J Oncol. 57 (6) (2020) 1333–1347, https://doi.org/10.3892/ijo.2020.5142.
[23] Xue L, Li J, Lin Y, Liu D, Yang Q, Jian J, et al. m^6 A transferase METTL3-induced lncRNA ABHD11-AS1 promotes the Warburg effect of non-small-cell lung cancer. J Cell Physiol. 236 (4) (2021) 2649–2658, https://doi.org/10.1002/jcp.30023.
[24] Li R, Yang YE, Yin YH, Zhang MY, Li H, Qu YQ. Methylation and transcriptome analysis reveal lung adenocarcinoma-specific diagnostic biomarkers. J Transl Med. 17 (1) (2019) 324, https://doi.org/10.1186/s12967-019-2068-z.
[25] Bader JE, Voss K, Rathmell JC. Targeting Metabolism to Improve the Tumor Microenvironment for Cancer Immunotherapy. Mol Cell. 78 (6) (2020) 1019–1033, https://doi.org/10.1016/j.molcel.2020.05.034.
[26] Roma-Rodrigues C, Mendes R, Baptista PV, Fernandes AR. Targeting Tumor Microenvironment for Cancer Therapy. Int J Mol Sci. 20 (4) (2019) 840, https://doi.org/10.3390/ijms20040840.
[27] Meurette O, Mehlen P. Notch Signaling in the Tumor Microenvironment. Cancer Cell. 34 (4) (2018) 536–548, https://doi.org/10.1016/j.ccell.2018.07.009.
[28] Wang Z, Zhao Y, Zhang L. Emerging trends and hot topics in the application of multi-omics in drug discovery: A bibliometric and visualized study. Current Pharmaceutical Analysis. 21 (2024) 20–32, https://doi.org/10.1016/j.cpan.2024.12.001.
[29] Pitt JM, Marabelle A, Eggermont A, Soria JC, Kroemer G, Zitvogel L. Targeting the tumor microenvironment: removing obstruction to anticancer immune responses and immunotherapy. Ann Oncol. 27 (8) (2016) 1482–1492, https://doi.org/10.1093/annonc/mdw168.
[30] Jin MZ, Jin WL. The updated landscape of tumor microenvironment and drug repurposing. Signal Transduct Target Ther. 5 (1) (2020) 166, https://doi.org/10.1038/s41392-020-00280-x.
[31] Chen D, Zhang X, Li Z, Zhu B. Metabolic regulatory crosstalk between tumor microenvironment and tumor-associated macrophages. Theranostics. 11 (3) (2021) 1016–1030,

https://doi.org/10.7150/thno.51777.
[32] Chen S, Crabill GA, Pritchard TS, McMiller TL, Wei P, Pardoll DM, et al. Mechanisms regulating PD-L1 expression on tumor and immune cells. J Immunother Cancer. 7 (1) (2019) 305, https://doi.org/10.1186/s40425-019-0770-2.
[33] Chen B, Gao A, Tu B, Wang Y, Yu X, Wang Y, et al. Metabolic modulation via mTOR pathway and anti-angiogenesis remodels tumor microenvironment using PD-L1-targeting codelivery. Biomaterials. 255 (2020) 120187, https://doi.org/10.1016/j.biomaterials.2020.120187.
[34] He L, Li H, Wu A, Peng Y, Shu G, Yin G. Functions of N6-methyladenosine and its role in cancer. Mol Cancer. 18 (1) (2019) 176, https://doi.org/10.1186/s12943-019-1109-9.
[35] Dorn LE, Lasman L, Chen J, Xu X, Hund TJ, Medvedovic M, et al. The N^6-Methyladenosine mRNA Methylase METTL3 Controls Cardiac Homeostasis and Hypertrophy. Circulation. 139 (4) (2019) 533–545, https://doi.org/10.1161/CIRCULATIONAHA.118.036146.
[36] Huang GZ, Wu QQ, Zheng ZN, Shao TR, Lv XZ. Identification of Candidate Biomarkers and Analysis of Prognostic Values in Oral Squamous Cell Carcinoma. Front Oncol. 9 (2019) 1054, https://doi.org/10.3389/fonc.2019.01054.
[37] He R, Man C, Huang J, He L, Wang X, Lang Y, et al. Identification of RNA Methylation-Related lncRNAs Signature for Predicting Hot. Identification of RNA Methylation-Related lncRNAs Signature for Predicting Hot and Cold Tumors and Prognosis in Colon Cancer. Front Genet. 13 (2022) 870945, https://doi.org/10.3389/fgene.2022.870945.
[38] Hess AS, Hess JR. Kaplan-Meier survival curves. Transfusion. 60 (4) (2020) 670–672, https://doi.org/10.1111/trf.15725.
[39] Frankish A, Diekhans M, Jungreis I, Lagarde J, Loveland JE, Mudge JM, et al. GENCODE 2021. Nucleic Acids Res. 49 (D1) (2021) D916–D923, https://doi.org/10.1093/nar/gkaa1087.
[40] Biscay Lirio R, Valdés Sosa PA, Pascual Marqui RD, Jiménez-Sobrino JC, Alvarez Amador A, Galán Garcia L. Multivariate Box-Cox transformations with applications to neurometric data. Comput Biol Med. 19 (4) (1989) 263–267, https://doi.org/10.1016/0010-4825(89)90013-9.
[41] Park SY. Nomogram: An analogue tool to deliver digital knowledge. J Thorac Cardiovasc Surg. 155 (4) (2018) 1793, https://doi.org/10.1016/j.jtcvs.2017.12.107.
[42] Heagerty PJ, Zheng Y. Survival model predictive accuracy and ROC curves. Biometrics. 61 (1) (2005) 92–105, https://doi.org/10.1111/j.0006-341X.2005.030814.x.
[43] Osterman TJ, Terry M, Miller RS. Improving Cancer Data Interoperability: The Promise of the Minimal Common Oncology Data Elements (mCODE) Initiative. JCO Clin Cancer Inform. 4 (2020) 993–1001, https://doi.org/10.1200/CCI.20.00059.
[44] Chin CH, Chen SH, Wu HH, Ho CW, Ko MT, Lin CY. cytoHubba: identifying hub objects and sub-networks from complex interactome. BMC Syst Biol. 8 Suppl 4 (2014) S11, https://doi.org/10.1186/1752-0509-8-S4-S11.
[45] Powers RK, Goodspeed A, Pielke-Lombardo H, Tan AC, Costello JC. GSEA-InContext: identifying novel and common patterns in expression experiments. Bioinformatics. 34 (13) (2018) i555–i564, https://doi.org/10.1093/bioinformatics/bty271.
[46] Gene Ontology Consortium: going forward. Nucleic Acids Res. 43 (Database issue) (2015) D1049–D1056, https://doi.org/10.1093/nar/gku1179.
[47] Kanehisa M, Goto S. KEGG: kyoto encyclopedia of genes and genomes. Nucleic Acids Res. 28 (1) (2000) 27–30, https://doi.org/10.1093/nar/28.1.27.
[48] Wilkerson MD, Hayes DN. ConsensusClusterPlus: a class discovery tool with confidence

assessments and item tracking. Bioinformatics. 26 (12) (2010) 1572–1573, https://doi.org/10.1093/bioinformatics/btq170.
[49] Chen B, Khodadoust MS, Liu CL, Newman AM, Alizadeh AA. Profiling Tumor Infiltrating Immune Cells with CIBERSORT. Methods Mol Biol. 1711 (2018) 243–259, https://doi.org/10.1007/978-1-4939-7493-1_12.
[50] Wu J, Li L, Zhang H, Zhao Y, Zhang H, Wu S, et al. A risk model developed based on tumor microenvironment predicts overall survival and associates with tumor immunity of patients with lung adenocarcinoma. Oncogene. 40 (26) (2021) 4413–4424, https://doi.org/10.1038/s41388-021-01853-y.
[51] Sung H, Ferlay J, Siegel RL, Laversanne M, Soerjomataram I, Jemal A, et al. Global Cancer Statistics 2020: GLOBOCAN Estimates of Incidence and Mortality Worldwide for 36 Cancers in 185 Countries. CA Cancer J Clin. 71 (3) (2021) 209–249, https://doi.org/10.3322/caac.21660.
[52] Nagini S. Breast Cancer: Current Molecular Therapeutic Targets and New Players. Anticancer Agents Med Chem. 17 (2) (2017) 152–163, https://doi.org/10.2174/1871520616666160502122724.
[53] Chen L, Huang S, Huang J, Chen Q, Zhuang Q. Role and Mechanism of Exosome-Derived Long Noncoding RNA HOTAIR in Lung Cancer. ACS Omega. 6 (27) (2021) 17217–17227, https://doi.org/10.1021/acsomega.1c00905.
[54] Fu Y, Dominissini D, Rechavi G, He C. Gene expression regulation mediated through reversible m^{6}A RNA methylation. Nat Rev Genet. 15 (5) (2014) 293–306, https://doi.org/10.1038/nrg3724.
[55] Seo KW, Kleiner RE. Mechanisms of epitranscriptomic gene regulation. Biopolymers. 112 (1) (2021) e23403, https://doi.org/10.1002/bip.23403.
[56] Darılmaz Yüce G, Ortaç Ersoy E. Lung cancer and epigenetic modifications. Tuberk Toraks. 64 (2) (2016) 163–170, https://doi.org/10.5578/tt.10231.
[57] Li B, Zhu L, Lu C, Wang C, Wang H, Jin H, et al. circNDUFB2 inhibits non-small cell lung cancer progression via destabilizing IGF2BPs and activating anti-tumor immunity. Nat Commun. 12 (1) (2021) 295, https://doi.org/10.1038/s41467-020-20527-z.
[58] Guo YP, Wang ZF, Li N, Lei QQ, Cheng Q, Shi LG, et al. Suppression of lncRNA HOTAIR alleviates RCC angiogenesis through regulating miR-126/EGFL7 axis. Am J Physiol Cell Physiol. 320 (5) (2021) C880–C891, https://doi.org/10.1152/ajpcell.00459.2019.
[59] Dong J, Li B, Lin D, Zhou Q, Huang D. Advances in Targeted Therapy and Immunotherapy for Non-small Cell Lung Cancer Based on Accurate Molecular Typing. Front Pharmacol. 10 (2019) 230, https://doi.org/10.3389/fphar.2019.00230.
[60] Wang J, Tian X, Han R, Zhang X, Wang X, Shen H, et al. Downregulation of miR-486-5p contributes to tumor progression and metastasis by targeting protumorigenic ARHGAP5 in lung cancer. Oncogene. 33 (9) (2014) 1181–1189, https://doi.org/10.1038/onc.2013.42.
[61] Kim-Wanner SZ, Assenov Y, Nair MB, Weichenhan D, Benner A, Becker N, et al. Genome-Wide DNA Methylation Profiling in Early Stage I Lung Adenocarcinoma Reveals Predictive Aberrant Methylation in the Promoter Region of the Long Noncoding RNA PLUT: An Exploratory Study. J Thorac Oncol. 15 (8) (2020) 1338–1350, https://doi.org/10.1016/j.jtho.2020.03.023.
[62] Li JP, Li R, Liu X, Huo C, Liu TT, Yao J, et al. A Seven Immune-Related lncRNAs Model to Increase the Predicted Value of Lung Adenocarcinoma. Front Oncol. 10 (2020) 560779,

https://doi.org/10.3389/fonc.2020.560779.
[63] Lu S, Shan N, Chen X, Peng F, Wang Y, Long H. A novel immune-related long non-coding RNAs risk model for prognosis assessment of lung adenocarcinoma. Aging (Albany NY). 13 (23) (2021) 25550–25563, https://doi.org/10.18632/aging.203772.
[64] Shao J, Zhang B, Kuai L, Li Q. Integrated analysis of hypoxia-associated lncRNA signature to predict prognosis and immune microenvironment of lung adenocarcinoma patients. Bioengineered. 12 (1) (2021) 6186–6200, https://doi.org/10.1080/21655979.2021.1973874.
[65] Liu H, Zhang Q, Lou Q, Zhang X, Cui Y, Wang P, et al. Differential Analysis of lncRNA, miRNA and mRNA Expression Profiles and the Prognostic Value of lncRNA in Esophageal Cancer. Pathol Oncol Res. 26 (2) (2020) 1029–1039, https://doi.org/10.1007/s12253-019-00655-8.